Chapter

5.1 Electron Optics

Sol Sherr

Jerry C. Whitaker, Editor-in-Chief

5.1.1 Introduction

The electron gun is basic to the structure and operation of any cathode-ray device, specifically display devices. In its simplest schematic form, an electron gun may be represented by the diagram in Figure 5.1.1, which shows a triode gun in cross section. Electrons are emitted by the cathode, which is heated by the filament to a temperature sufficiently high to release the electrons. Because this stream of electrons emerges from the cathode as a cloud rather than a beam, it is necessary to accelerate, focus, deflect, and otherwise control the electron emission so that it becomes a beam, and can be made to strike a phosphor at the proper location, and with the desired beam cross section.

5.1.2 Electron Motion

The laws of motion for an electron in a uniform *electrostatic field* are obtained from Newton's second law. The velocity of an emitted electron is given by

$$v = \left\{\frac{2eV}{m}\right\}^{1/2} \tag{5.1.1}$$

Where:
$e = 1.6 \times 10^{-19} C$
$m = 9.1 \times 10^{-28} g$
$V = -Ex$, the potential through which the electron has fallen

When practical units are substituted for the values in the previous equation, the following results:

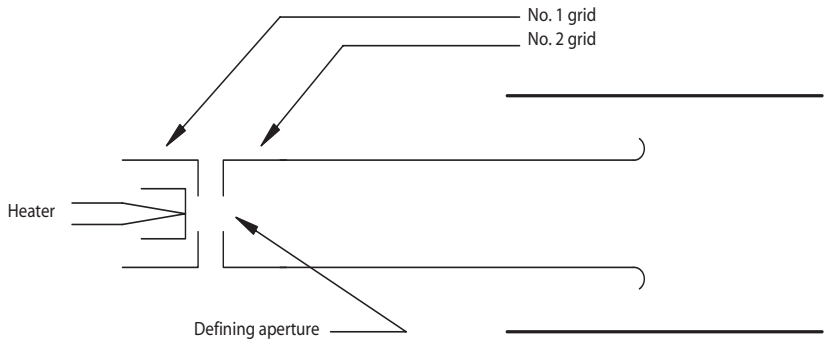

Figure 5.1.1 Triode electron gun structure.

$$v = 5.93 \times 10^5 V^{1/2} \quad \text{m/s} \tag{5.1.2}$$

This expression represents the velocity of the electron. If the electron velocity is at the angle θ to the potential gradient in a uniform field, the motion of the electron is specified by

$$y = -\frac{Ex^2}{4V_0 \sin^2 \theta} + \frac{x}{\tan \theta} \tag{5.1.3}$$

Where:
V_0 = the electron potential at initial velocity

This equation defines a parabola. The *electron trajectory* is illustrated in Figure 5.1.2, in which the following conditions apply:

- y_m = maximum height
- $x_m = x$ displacement at the maximum height
- α = the slope of the curve

5.1.2a Tetrode Gun

The tetrode electron gun includes a fourth electrode, illustrated in Figure 5.1.3. The main advantage of the additional electrode is improved convergence of the emitted beam.

Operating Principles

Nearly all currently available CRT electron guns have indirectly heated cathodes in the form of a small capped nickel sleeve or cylinder with an insulated coiled tungsten heater inserted from the

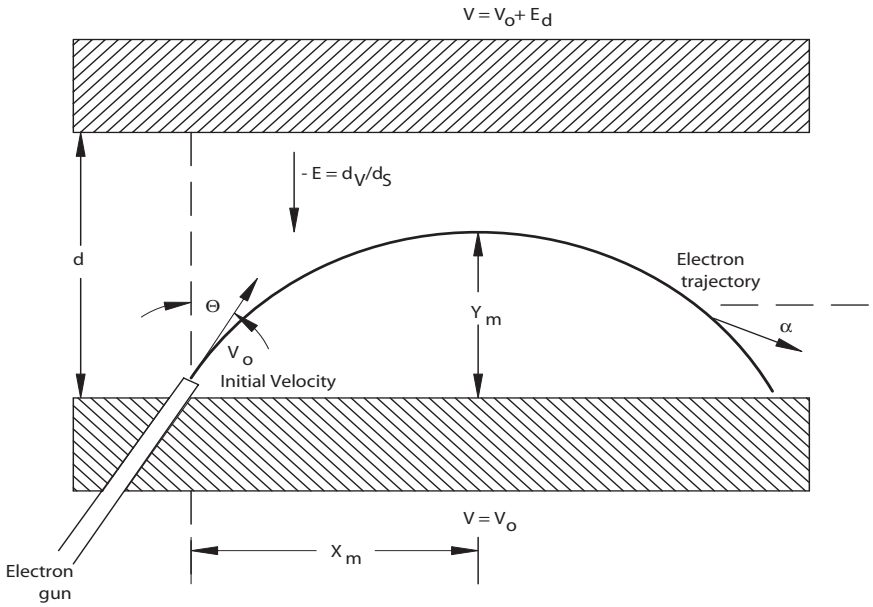

Figure 5.1.2 The electron trajectory from an electron gun using the parameters specified in the text. (*After* [1].)

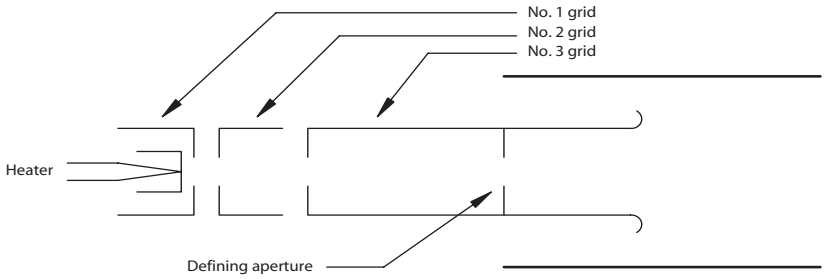

Figure 5.1.3 Basic structure of the tetrode electron gun.

back end. Most heaters operate at 6.3 Vac at a current of 300 to 600 mA. Low-power heaters are also available that operated at 1.5 V (typically 140 mA).

The cathode assembly is mounted on the axis of the modulating or *control grid* cylinder (or simply *grid*), which is a metal cup of low-permeability or stainless steel about 0.5-in in diameter and 0.375- to 0.5-in long. A small aperture is punched or drilled in the cap. The grid (G_1) voltage is usually negative with respect to the cathode (K).

To obtain electron current from the cathode through the grid aperture, there must be another electrode beyond the aperture at a positive potential great enough for its electrostatic field to

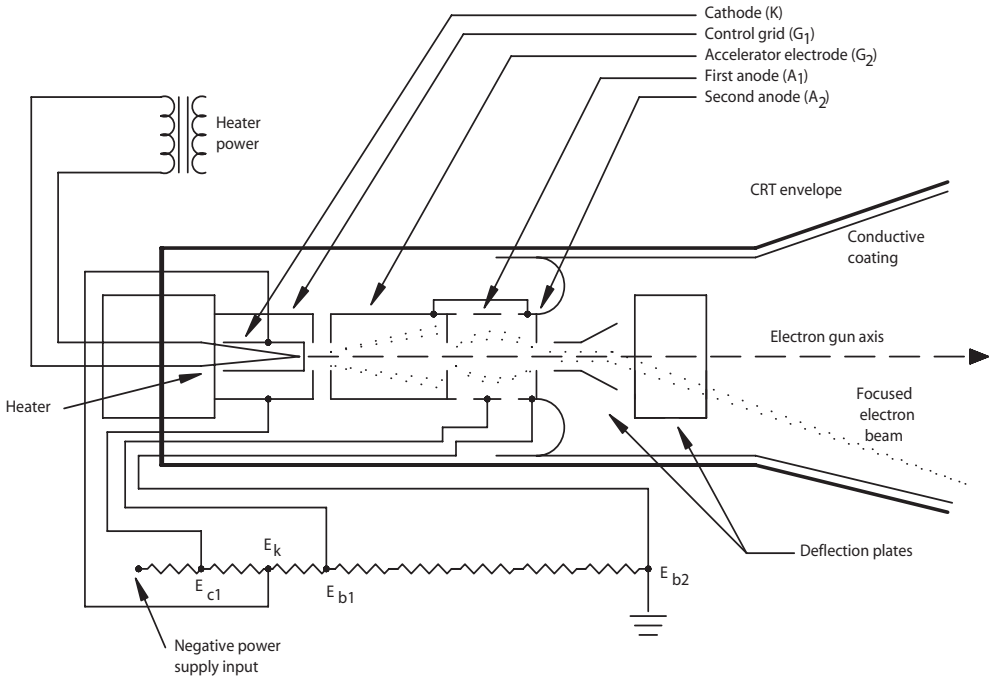

Figure 5.1.4 Generalized schematic of a CRT grid structure and accelerating electrode in a device using electrostatic deflection.

penetrate the aperture to the cathode surface. Figure 5.1.4 illustrates a typical *accelerating electrode* (G_2) in relation to the cathode structure. The accelerating electrode may be implemented in any given device in a number of ways. In a simple accelerating lens in which successive electrodes have progressively higher voltages, the electrode may also be used for focusing the electron beam upon the phosphor, hence, it may be designated the *focusing* (or *first*) anode (A_1). This element is usually a cylinder, longer than its diameter and probably containing one or more disk apertures.

5.1.2b Electron Beam Focusing

General principles involved in focusing the electron beam are best understood by initially examining optical lenses and then establishing the parallelism between them and electrical focusing techniques.

Electrostatic Lens

Figure 5.1.5 shows a simplified diagram of an electrostatic lens. An electron emitted at zero velocity enters the V_1 region moving at a constant velocity (because the region has a constant potential). The velocity of the electron in that region is defined by equation (5.1.2) for the

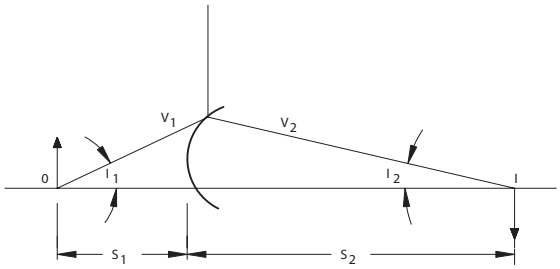

Figure 5.1.5 The basic principles of electron optics. (*After* [2].)

straight-line component, with V_1 replacing V. After passing through the surface into the V_2 region, the velocity changes to a new value determined by V_2. The only component of the velocity that is changed is the one normal to the surface, so that the following conditions are true:

$$v_t = v_1 \sin I_1 \tag{5.1.4}$$

$$v_1 \sin I_1 = v_2 \sin I_2 \tag{5.1.5}$$

Snell's law, also known as the law of refraction, has the form

$$N_1 \sin I_1 = N_2 I_2 \tag{5.1.6}$$

Where:
N_1 = the index of refraction for the first medium
N_2 = the index of refraction for the second medium
I_1 = the angle of the incident ray with the surface normal
I_2 = the angle of the refracted ray with the surface normal

The parallelism between the optical and the electrostatic lens is apparent if appropriate substitutions are made

$$V_1 \sin I_1 = V_2 \sin I_2 \tag{5.1.7a}$$

$$\frac{\sin I_1}{\sin I_2} = \frac{V_2}{V_1} \tag{5.1.7b}$$

For Snell's law, the following applies:

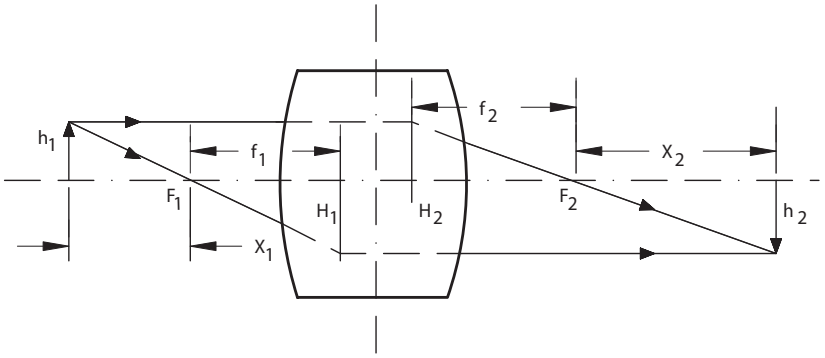

Figure 5.1.6 A unipotential lens. (*After* [2].)

$$\frac{\sin I_1}{\sin I_2} = \frac{N_2}{N_1} \tag{5.1.8}$$

Thus, the analogy between the optical lens and the electrostatic lens is apparent. The magnification m of the electrostatic lens is given by

$$m = \frac{\left\{V_1 / V_2\right\}^{1/2} S_2}{S_1} \tag{5.1.9}$$

(Symbols defined in Figure 5.1.5.)

The condition of a thin, *unipotential lens*, where V_1 is equal to V_2, is illustrated in Figure 5.1.6. The following applies:

$$m = \frac{h_2}{h_1} = \frac{f_2}{X_1} = -\frac{X_2}{f_2} \tag{5.1.10}$$

The shape of the electron beam under the foregoing conditions is shown in Figure 5.1.7. If the potential at the screen is the same as the potential at the anode, the crossover is imaged at the screen with the magnification given by

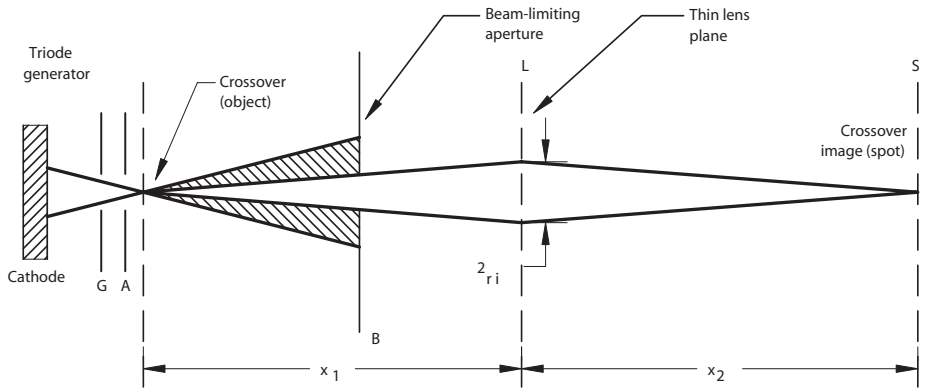

Figure 5.1.7 Electron beam shape. (*After* [3].)

$$m = \frac{x_2}{x_1} \tag{5.1.11}$$

The magnification can be controlled by changing this ratio, which, in turn, changes the size of the spot. This is one way to control the quality of the focus. Although the actual lens may not be "thin," and, in general, is more complicated than what is shown in the figure, the illustration is sufficient for understanding the operation of electrostatic focus.

The size of the spot can be controlled by changing the ratio of V_1 to V_2 or of x_2 to x_1 in the previous equations. Because x_1 and x_2 are established by the design of the CRT, the voltage ratio is the parameter available to the circuit designer to control the size or focus of the spot. It is by this means that focusing is achieved for CRTs using electrostatic control.

Practical Applications

Figure 5.1.8 illustrates a common type of gun and focusing system that employs a screen grid (G_2), usually in the form of a short cup with an aperture facing the grid aperture. The voltage is usually maintained between 200 and 400 V positive. In an electrostatically focused electron gun, the screen grid is usually followed by the focusing anode. In a magnetically focused electron gun, the screen grid may be followed directly by the final anode.

In another type of electrostatically focused electron gun (illustrated in Figure 5.1.9) the grid is followed immediately by a long-apertured cylinder at the voltage of the principal anode (A_2). This element, called the *accelerator* or *preaccelerator*, is followed, in sequence, by either two short cylindrical electrodes or apertured disks. The last electrode and preaccelerator are connected within the tube. This set of three electrodes constitutes an *Einzel lens*. By proper design of the lens, the focal condition can be made to occur when the voltage on the central element is zero or a small positive voltage with reference to the cathode.

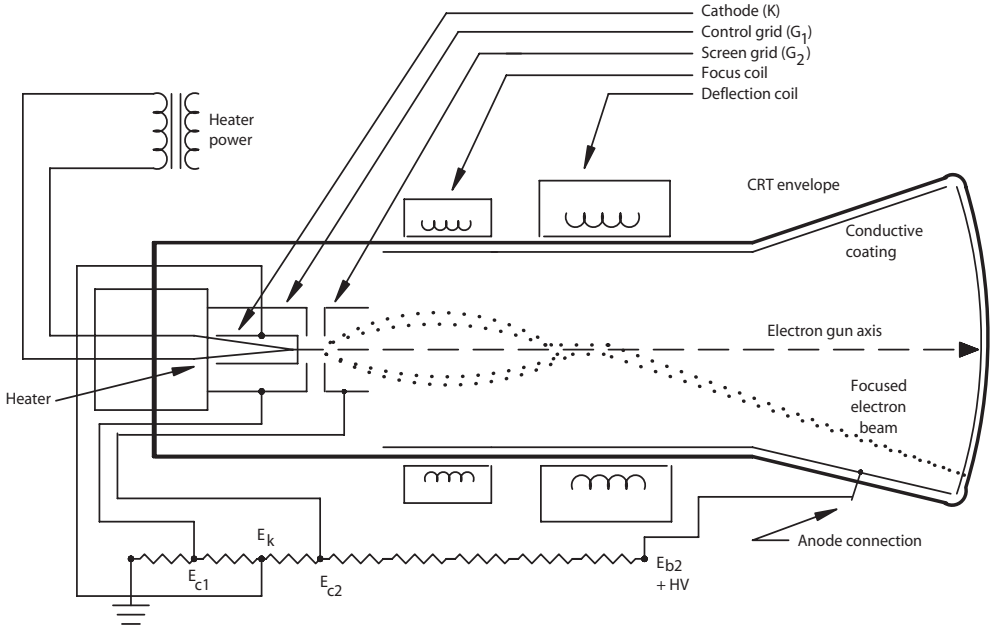

Figure 5.1.8 Generalized schematic of a CRT gun structure using electromagnetic focus and deflection. (*After* [4].)

5.1.2c Electrostatic Lens Aberrations

There are five common types of aberrations associated with electrostatic lenses for single beam guns and an additional aberration associated with multi-beam guns:

- Astigmatism
- Coma
- Curvature of field
- Distortion of field
- Spherical aberration
- Chromatic aberration (for a multi-beam (color) systems)

Chromatic aberration, illustrated in Figure 5.1.10, is analogous to the effect in geometrical optics resulting in light of different wavelengths having different focal lengths. In an electrostatic lens, electrons with different velocities will have different focal points. However, because electron velocity is different only insofar as the electrons leave the cathode with different emission velocities, the effect is generally small at the accelerating potentials that are used, and the error is usually not significant.

Coma applies to images and objects not on the axis of the lens system. Figure 5.1.11 illustrates circles imaged in a distorted form. Coma may be reduced by using less of the lens center,

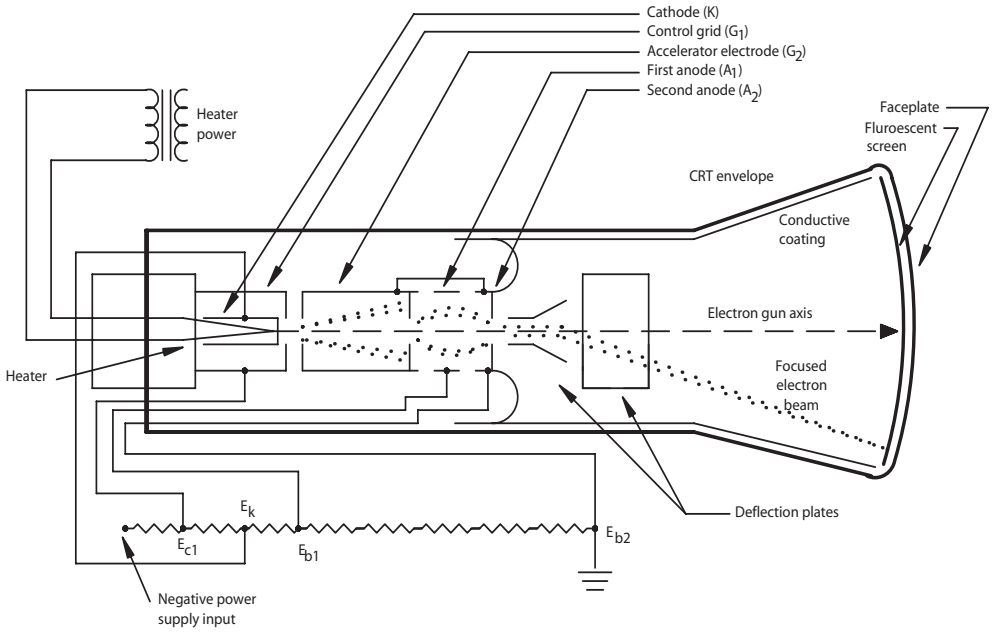

Figure 5.1.9 Generalized schematic of a CRT with electrostatic focus and deflection. An Einzell focusing lens is depicted. (*After* [4].)

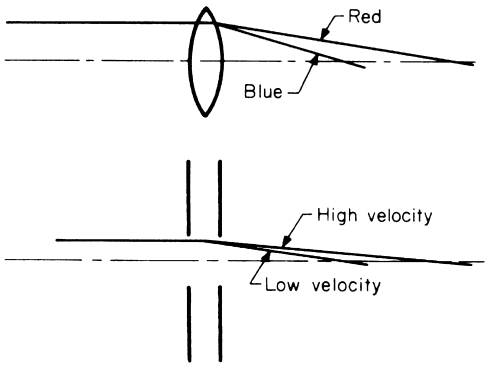

Figure 5.1.10 Illustration of chromatic aberration. (*After* [1].)

but this reduces the amount of beam current and, therefore, available luminance; it may not be a desirable approach.

Astigmatism results from objects positioned off the axis lines toward the axis having different focal lengths than lines that are perpendicular to them. This effect is well known in geometrical optics and is shown in Figure 5.1.12. From this figure it can be seen that compromises must be made when focusing the entire image. Changing the focusing voltage changes the portion of the image that is sharply focused, while the rest of the image may be blurred.

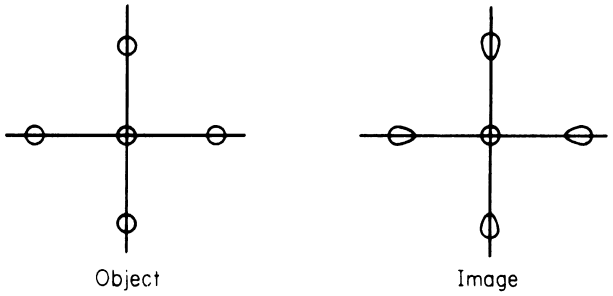

Figure 5.1.11 Illustration of coma. (*After* [1].)

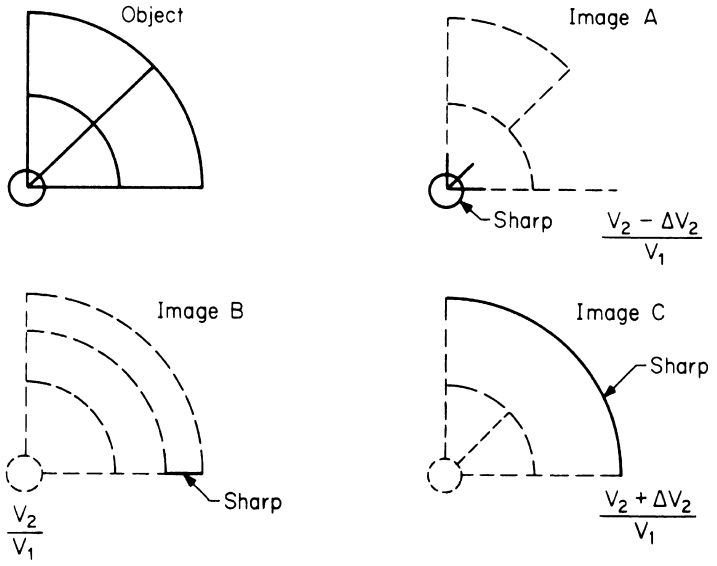

Figure 5.1.12 Illustration of astigmatism. (*After* [1].

Curvature of field is usually associated with astigmatism but is a more noticeable effect, resulting from the image lying on a curved surface for an object that is in a plane at right angles to the axis. This results in concentric circles that can be adjusted in the image plane so only one radial distance is sharp. Thus, if the center is focused, the outside will be unfocused, or the opposite, if the outer circle is focused.

Distortion of field results from variations in linear magnification with the radial distance. These are the well-known *pincushion* and *barrel* distortions; the former results from an increase in magnification and the latter from a decrease. The distortions are illustrated in Figure 5.1.13.

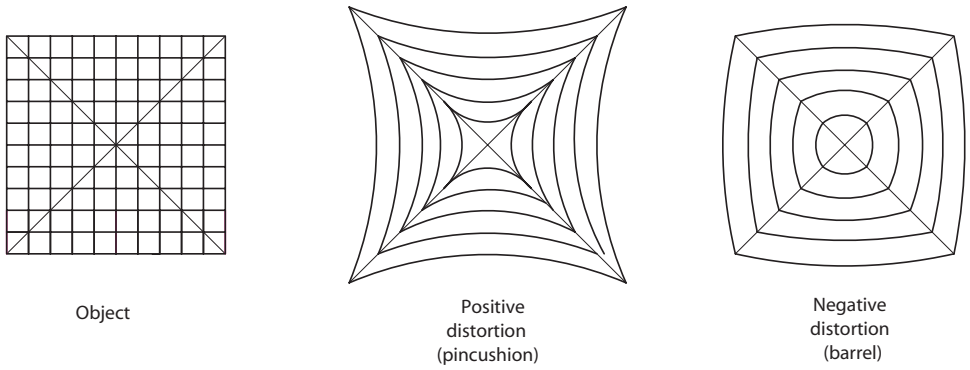

Figure 5.1.13 Pincushion and barrel distortion. (*After* [1].)

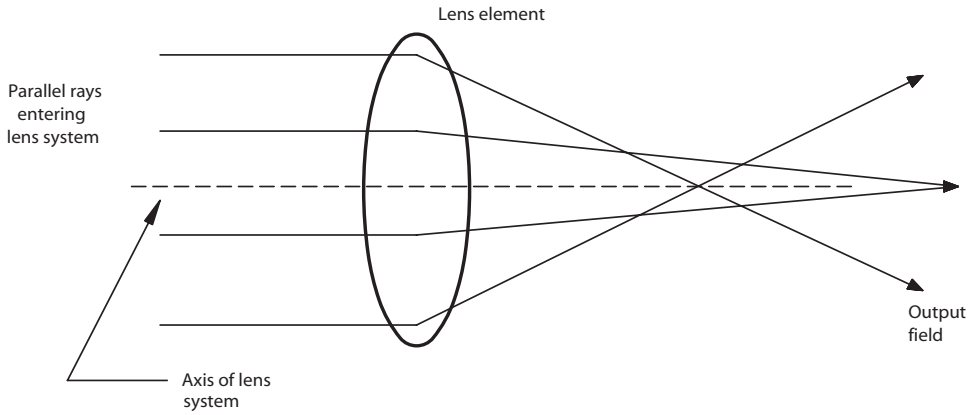

Figure 5.1.14 Spherical aberration. (*After* [5].)

Spherical aberration is a distortion where parallel rays entering the lens system have different focal lengths depending on the radial distance of the ray from the center of the lens. This effect is shown in Figure 5.1.14. It is perhaps the most serious of all the aberrations. It can be seen from the figure that the focal length becomes smaller as the distance increases. This is known as *positive spherical aberration* and is always found when electron lenses are used. The focal length increases slowly at first, and then more rapidly as the radial distance increases. This type of aberration is always positive in electron lenses, and cannot be eliminated by adding a lens with equal *negative spherical aberration*, as is the case with optical systems. However, it is possible to reduce the effect somewhat by using dual-cylinder lenses with a high-potential inner cylinder and a lower-potential outer cylinder.

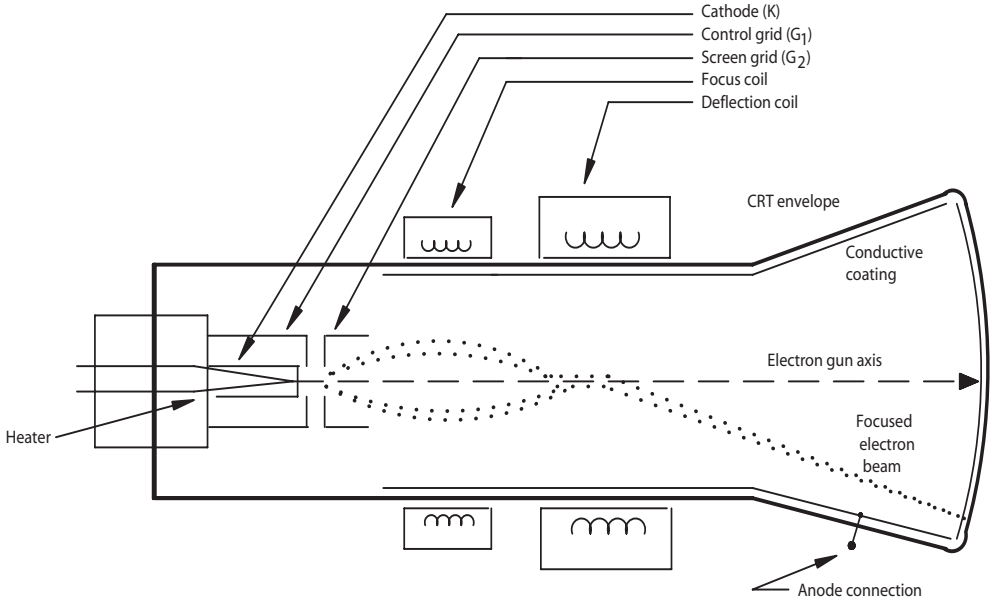

Figure 5.1.15 Magnetic-focusing elements on the neck of a CRT.

5.1.2d Magnetic Focusing

It is well known that electron beams can be focused with magnetic fields as well as with electrostatic fields, but the analogy with optical systems is not as apparent. When electrons leave a point on a source with the principal component of the velocity parallel to the axis of a long magnetic field, they travel in helical paths and come to a focus at a further point along the axis. The helical paths have essentially the same pitch. Supporting equations show that the pitch is relatively insensitive to θ for small angles, and the electrons will return to their original relative positions at some distance *P* on the magnetic path that is parallel to the electron beam. Thus, spreading of the beam is avoided, but there is no reduction in the initial beam diameter. Focusing is achieved by changing the current in the focusing coil until the best spot size is achieved. The manner in which the focus coil is placed around the neck of the CRT is shown in Figure 5.1.15. The focal length of such a coil is given by [6]

$$f = \frac{4.86Vd}{N^2 I^2} \tag{5.1.12}$$

Where:
f = focal length
d =diameter of wire loop
NI = current in ampere-turns

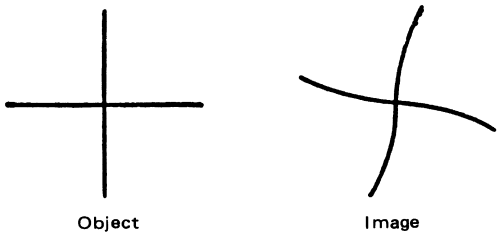

Figure 5.1.16 Spiral distortion in magnetic-lens images. (*After* [1].)

V = potential of region

This equation can be used for a short coil with a mean diameter of d that has N turns and a current equal to I.

The image rotation θ is expressed by

$$\theta = \frac{0.19NI}{V^{1/2}} \tag{5.1.13}$$

Practical Applications

Magnetic focusing is rarely used in common video displays; the majority of CRTs are designed with electrostatic focus elements. Magnetic focusing, however, can provide superior resolution compared with electrostatic focusing. The gun structure is simpler than what is needed for electrostatic focusing. Only the cathode, control electrode, and accelerating electrode are required, with the focus coil usually located externally on the neck of the CRT. A constant current source must be provided for the magnetic focus coil, which can be varied to control the focal point.

A common method of magnetic focusing employs a short magnetic lens that operates by means of the radial inhomogeneity of the magnetic field, and can have both the object and image points distant from the lens. The typical short magnetic lens or focus coil consists of a large number of turns of fine wire with a total resistance of several hundred ohms, wound on a bobbin of insulating paper or plastic. The bobbin and coil are almost totally enclosed in a soft-iron shell, except for an annular gap of about 0.375-in at one end of the core tubing.

5.1.2e Magnetic Lens Aberrations

A magnetic lens is subject to the same aberrations as an electrostatic lens. A magnetic lens may also suffer from an additional distortion that is associated with the rotation of the image. This distortion is called *spiral distortion* and is illustrated in Figure 5.1.16. Spiral distortion results from different parts of the image being rotated different amounts as a function of their radial position. The effect is reduced by using very small apertures, or is essentially eliminated by having a pair of lenses that rotate in different directions. There is also the possibility of distortion resulting from stray fields or ripple in the current driving the focus coil. Current ripple causes a point to become a blurred spot, whereas stray fields cause a point to elongate to a line. Both of

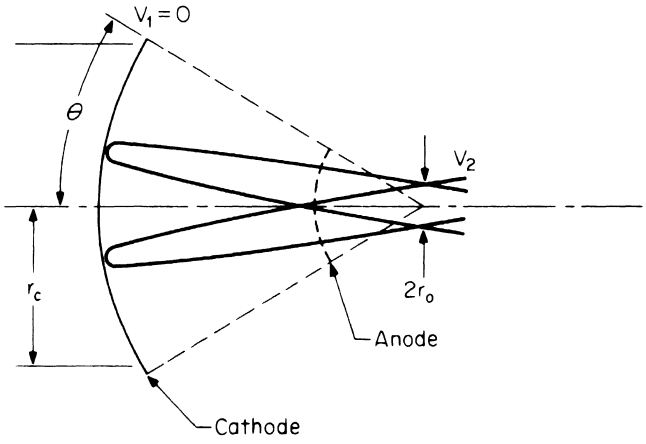

Figure 5.1.17 Idealized cathode with a spherical field. (*After* [1].)

these effects can be minimized by careful design of the current source and the focus coil, respectively.

5.1.2f Beam Crossover

The *beam crossover* is used as the object whose image appears on the screen of the CRT. Therefore, the location and size of the crossover are important in determining the minimum spot size attainable by means of the focusing techniques previously described in this section. While the exact values are difficult to determine, a good approximation can be achieved by assuming a spherical field in the vicinity of the cathode. This idealized arrangement is shown in Figure 5.1.17. The radius of the crossover is given by [1]

$$r_0 = \frac{2r_c}{\sin 2\theta \left\{ V_2 / V_e \right\}^{1/2}} \tag{5.1.14}$$

Where:
r_0 = the crossover radius
r_c = the crossover potential
V_2 = the crossover potential
V_e = voltage equivalent of emission velocity
θ = cathode half-angle viewed from the crossover

The crossover radius changes for different velocities of emission. Therefore, because the electrons will be emitted at all possible velocities, an average value of V_e must be used. In addition, the equation is valid only for small values of θ (less than 20°). It should be noted that these effects are controlled by the tube design and are not available for user manipulation after a given CRT has been selected.

A variety of techniques can be used to correct for lens aberrations. While such correction is commonly used—and in some cases is unavoidable—it is accepted practice that the less correction applied to the device, the better. Lens correction should be used to offset the unavoidable distortions resulting from electron optics, not manufacturing tolerances in the electron gun and deflection systems.

5.1.3 References

1. Spangenberg, K. R.: *Vacuum Tubes*, McGraw-Hill, New York, N.Y., 1948.
2. Sherr, S.: *Electronic Displays*, Wiley, New York, N.Y., 1979.
3. Moss, Hilary: *Narrow Angle Electron Guns and Cathode Ray Tubes*, Academic, New York, N.Y., 1968.
4. *Cathode Ray Tube Displays*, MIT Radiation Laboratory Series, vol. 22, McGraw-Hill, New York, N.Y., 1953.
5. Zworykin, V. K., and G. Morton: *Television*, 2d ed., Wiley, New York, N.Y., 1954.
6. Pender, H., and K. McIlwain (eds.): *Electrical Engineers Handbook*, Wiley, New York, N.Y., 1950.

5.1.4 Bibliography

Boers, J.: "Computer Simulation of Space Charge Flows," Rome Air Development Command RADC-TR-68-175, University of Michigan, 1968.

Casteloano, Joseph A.: *Handbook of Display Technology*, Academic, New York, N.Y., 1992.

Fink, Donald, and Donald Christiansen (eds.): *Electronics Engineers Handbook*, 3rd ed., McGraw-Hill, New York, N.Y., 1989.

IEEE Standard Dictionary of Electrical and Electronics Terms, 2nd ed., Wiley, New York, N.Y., 1977.

Jordan, Edward C. (ed.): *Reference Data for Engineers: Radio, Electronics, Computer, and Communications*, 7th ed., Howard W. Sams, Indianapolis, IN, 1985.

Langmuir, D.: "Limitations of Cathode Ray Tubes," *Proc. IRE*, vol. 25, pp. 977–991, 1937.

Luxenberg, H. R., and R. L. Kuehn (eds.): *Display Systems Engineering*, McGraw-Hill, New York, N.Y., 1968.

Nix, L.: "Spot Growth Reduction in Bright, Wide Deflection Angle CRTs," *SID Proc*., Society for Information Display, San Jose, Calif., vol. 21, no. 4, pg. 315, 1980.

Poole, H. H.: *Fundamentals of Display Systems*, Spartan, Washington, D.C., 1966.

Sadowski, M.: *RCA Review*, vol 95, 1957.

Sherr, S.: *Fundamentals of Display Systems Design*, Wiley, New York, N.Y., 1970.

True, R.: "Space Charge Limited Beam Forming Systems Analyzed by the Method of Self-Consistent Fields with Solution of Poisson's Equation on a Deformable Relaxation Mesh," Ph.D. thesis, University of Connecticut, Storrs, 1968.

Chapter

5.2 Electrostatic Deflection

Sol Sherr

Jerry C. Whitaker, Editor-in-Chief

5.2.1 Introduction

An electrostatic deflection system generally consists of metallic deflection plates used in pairs within the neck of the CRT or other vacuum device. Table 5.2.1 compares the principle operating parameters of electromagnetic and electrostatic deflection CRTs. The first difference is the longer vacuum envelope required for the electrostatic type. This imposes packaging limitations on the assembly that contains the tube. Related to the increased length are the narrower deflection angles available in electrostatic types and the higher focus voltage required, as well as the need for a post-accelerator voltage. Of greatest significance, however, are the higher luminance and smaller spot size typically attainable with electromagnetic deflection. One characteristic not shown in the table is the faster deflection speed possible with the electrostatic deflection tube, which can be as low as 1 μs, compared with the 10 μs that is possible with a typical electromagnetic deflection tube. This parameter is not included because it is influenced by the choice of deflection amplifier and may be higher or lower, depending on the type of amplifier used. However, with the use of typical amplifier designs, the 10/1 advantage is not unusual.

5.2.2 Principles of Operation

Figure 5.2.1 shows the basic construction of an electrostatic deflection device. The simplest design incorporates flat rectangular parallel plates facing each other, with the electron beam directed along the central plane between them. The deflection plates are located in the field-free space within the second-anode region. The plates are essentially at second-anode voltage when no deflection signal is applied. Deflection of the electron beam is accomplished by establishing an electrostatic field between the plates.

Most electrostatic deflection devices do not exhibit excessive deflection defocusing until the beam deflection angle off-axis exceeds 20°. This limitation prevents the use of high deflection

Table 5.2.1 Comparison of Common Electromagnetic and Electrostatic Deflection CRTs

Parameter	Magnetic Deflection	Electrostatic Deflection
Deflection settling time	10 μs	< 1 μs to one spot diameter
Small-signal bandwidth	2 MHz	5 MHz
Video bandwidth	15–30 MHz	25 MHz
Linear writing speed	1 μs/cm	25 cm/μs
Resolution	1000 TV lines or more	17 lines/cm
Luminance	300 nits	150–500 nits
Spot size	0.25 mm (53 cm CRT)	0.25–0.38 mm
Accelerator voltage	10 kV	28 kV
Phosphor	Various	P-31 and others
Power consumption	250 W	130-140 W
Off-axis deflection	55°	20°
Physical length	Up to 30% shorter than electrostatic deflection	
Typical applications	Video display	Waveform display
1 nit = 1 candela per square meter (cd/m^2)		

angles common in magnetic deflection devices. Deflection angles of 55° off-axis are common in magnetic deflection CRTs.

Most electrostatic deflection CRTs are used to display electronic waveforms as a function of time. To accomplish this task, it is necessary to generate a sweep signal representing the passage of time, and to superimpose on the signal an orthogonal deflection representing signal amplitude. This is typically accomplished through the use of two pairs of deflection plates. The second pair of deflection plates must have a sufficiently wide entrance window to accept the maximum deflection of the beam produced by the first pair of plates. Design tradeoffs include overall deflection sensitivity and deflection plate capacitance. The plates (as shown in Figure 5.2.1) diverge to accommodate their own deflection of the electron beam. For a given deflection voltage, the magnitude of deflection is inversely proportional to the anode voltage.

5.2.2a Fundamental Principles

Figure 5.2.2 shows the basic arrangement of an electrostatic deflection CRT. Electron trajectory is illustrated in Figure 5.2.3. These figures provide the basis for deriving equations that describe the principles of operation for electrostatic deflection. Assuming that an electron enters the deflection field between the deflection plates at right angles (θ equal to 90°) then

$$\tan\theta = \frac{V_d\, d_l}{2 d_p\, V_b} \tag{5.2.1}$$

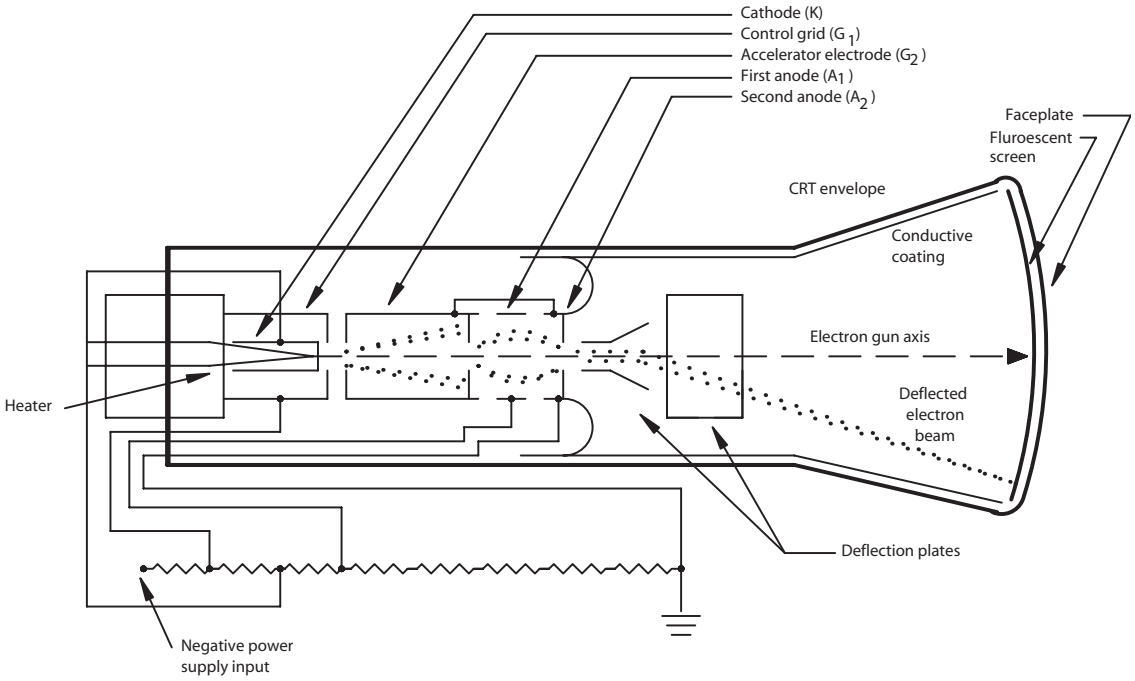

Figure 5.2.1 Electrostatic deflection CRT.

Where:
V_d = the voltage between the deflection plates
d_l = length of the plates
d_p = distance between the plates
V_b = beam voltage

Because the center of deflection is at the center of the field, tan θ is approximately equal to y_d/l, where y_d = the deflection distance and l = the length of the deflection field, shown in Figure 7.2(*b*). It follows, then

$$y_d = \frac{l\, d_l\, V_d}{2 d_p V_b} \tag{5.2.2}$$

This equation holds true for parallel plates and neglects fringe effects. For nonparallel plates, the gradient is [1]

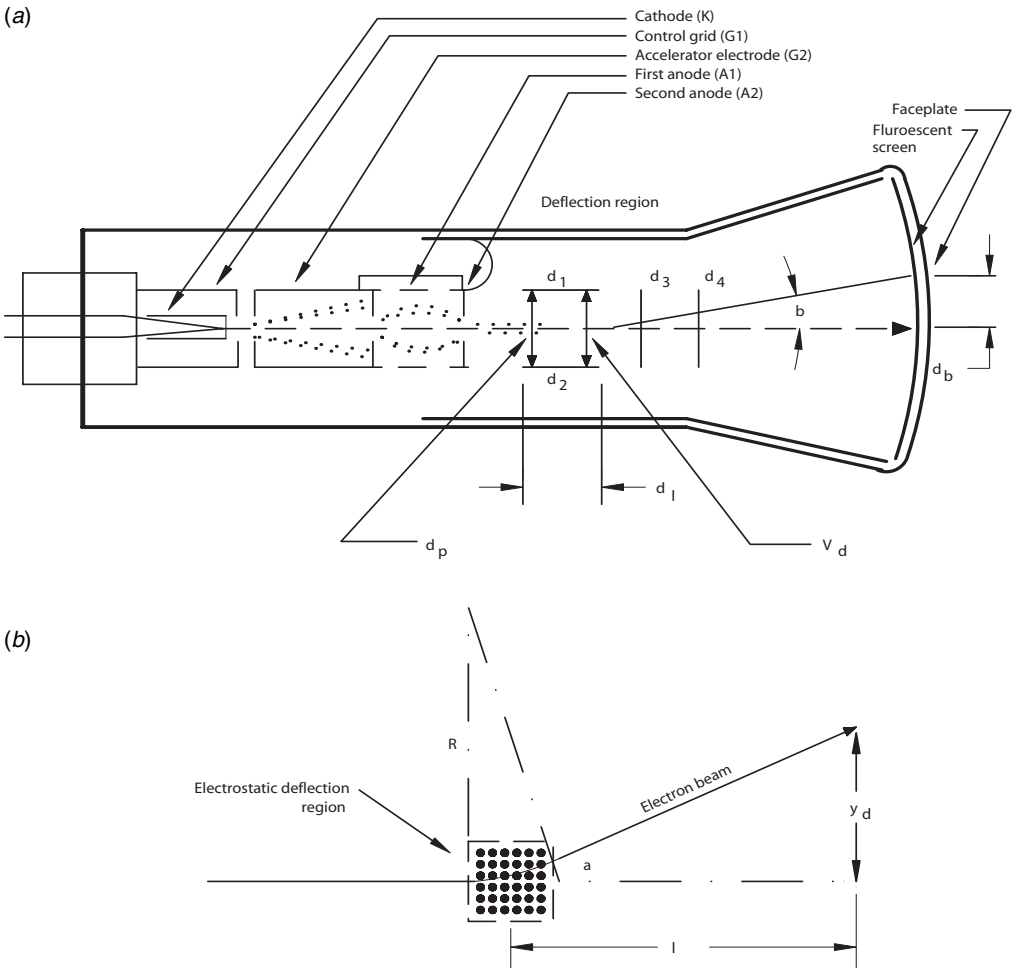

Figure 5.2.2 The elements of an electrostatic deflection CRT: (*a*) overall tube geometry, (*b*) detail of deflection region.

$$\frac{dv}{dy} = \frac{V_d}{a_1 + \left(a_2 - a_1\right)^{X/d_l}} \tag{5.2.3}$$

Where:
a_1 = plate separation at the entrance end
a_2 = plate separation at the departure end
X = distance for the beam in the field of the plates

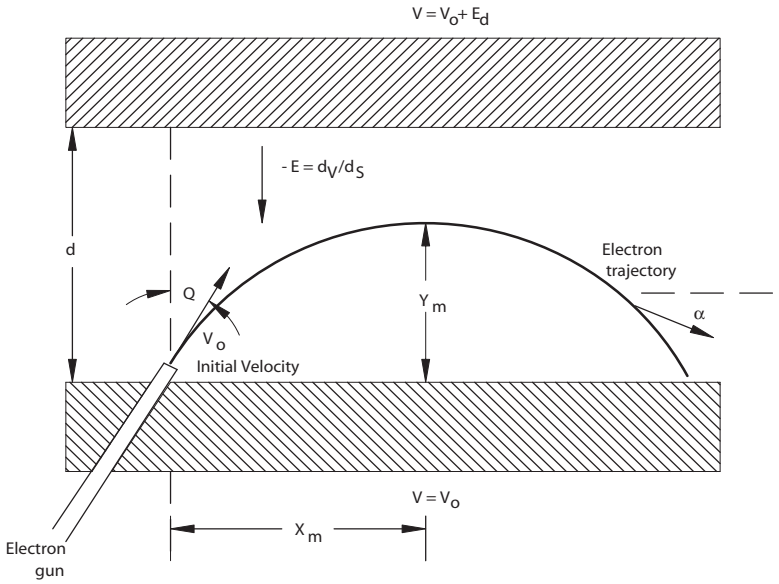

Figure 5.2.3 Trajectory of an electron beam. (*After* [1].)

The deflection equation then becomes [1]

$$y = \frac{d_l V_d}{2V_b a_1} \frac{ln\left\{a_2 \big/ a_1\right\}}{\left\{a_2 \big/ a_1\right\} - 1} \tag{5.2.4}$$

When a_1 is equal to a_2 (the plates are flat), the foregoing equation reduces to [1]

$$yd = \frac{l\, d_l V_d}{2 d_p V_b} \tag{5.2.5}$$

as shown previously.

5.2.2b Acceleration Voltage Effects

In an electrostatic deflection CRT, the deflection distance is directly proportional to the deflection voltage (V_d) and inversely proportional to the acceleration or beam voltage (V_b). This situa-

tion leads to the requirement that the deflection voltage must be increased a proportional amount when the beam voltage is increased. In an electromagnetic deflection CRT, deflection is proportional to the square root of the beam voltage. This leads to two considerations when electrostatic and magnetic deflection are compared. First, it can be shown that the beam spread as a function of beam voltage (in kilovolts) and current (in milliamperes) is given by [2]

$$K^{1/2} = \frac{32.2\, r_0\, V^{3/4}}{I^{1/2}} \tag{5.2.6}$$

Where:
V = beam voltage in kV
I = beam current in mA

This expression is represented in the nomograph shown in Figure 5.2.4, where r_0 = the *cross-over spot size* and z = the position of the beam. Based on the data presented, it is clear that the beam size is affected by the beam voltage, and the higher the beam voltage, the smaller the spot. However, increasing the beam voltage increases the required deflection voltage by a proportional amount, so that magnetic deflection can use larger beam voltages and, therefore, attain smaller spot sizes.

A second effect of beam voltage is that of light output from the phosphor, or luminance. Phosphor luminance is given by the empirical expression [3]

$$L = A\, f(p) V^n \tag{5.2.7}$$

Where
L = phosphor luminance
$f(p)$ = function of current
V = accelerating voltage
A = constant
n = 1.5 to 2

The phosphor output or luminance may also be expressed by

$$L = \frac{k_b\, I_b\, V_b{}^n}{A} \tag{5.2.8}$$

Where:
k_b = a proportionality factor termed *luminous efficiency*
I_b = beam current
V_b = beam voltage
A = the area of the phosphor surface

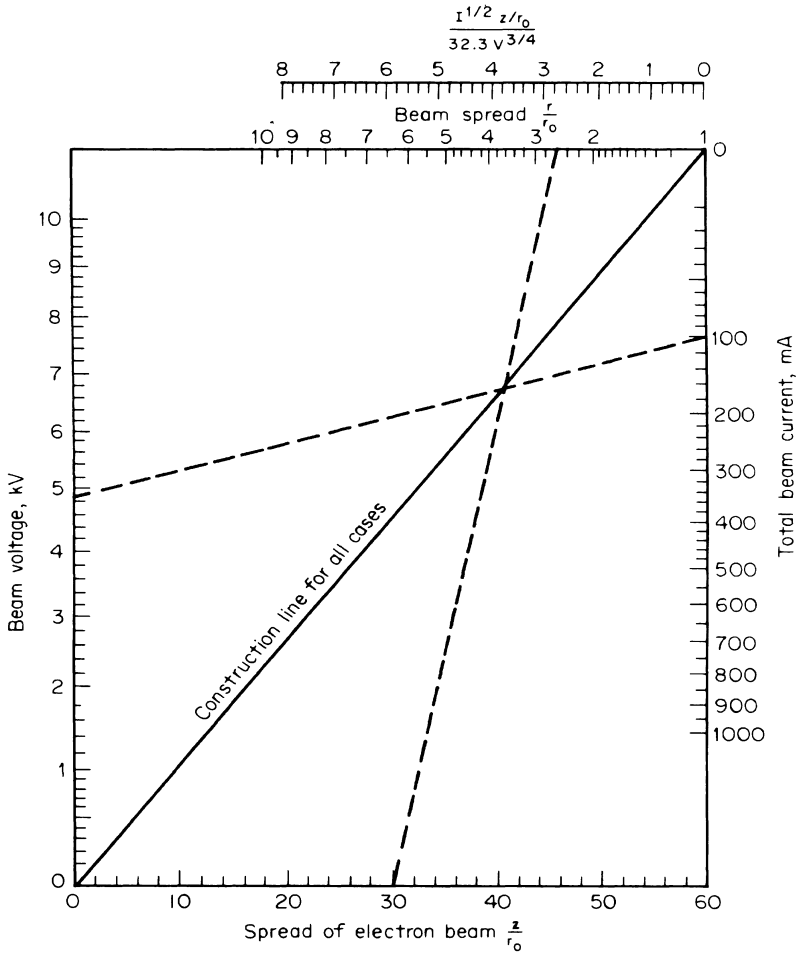

Figure 5.2.4 Beam spread nomograph.

The proportionality factor, which typically ranges from 5 to 62 for the various phosphors, is given in terms of lumens per watt.

The preceding equation clearly demonstrates the effect of beam voltage on light output and illustrates the desirability of maintaining the beam voltage at the highest value consistent with the other requirements, such as deflection sensitivity and focus voltage. The equation is approximately correct over the linear region, but does not hold true when phosphor saturation occurs. It is not possible, therefore, to increase phosphor luminance merely by raising the beam voltage.

5.2.2c Post-Deflection Accelerator

A post-deflection accelerator electrode is used in a number of electrostatic deflection CRTs. This element generally takes the form of a wide graphite band around the inside of the envelope funnel just behind the faceplate. It is usually connected to the aluminum film if the phosphor is aluminized. This element is also known as the *post-accelerator* or *third anode* (A_3).

The *spiral accelerator* is another type of post-deflection element. It can be used with a considerably higher A_3/A_2 voltage ratio without detrimental effects caused by the localized electron lens. The spiral accelerator consists of a high-resistance narrow circumferential spiral stripe of graphite of low screw pitch painted over a substantial length of the inside of the tube envelope funnel. The ends of the spiral are electrically connected to the A_2 and A_3 terminals. In operation, the spiral accelerator requires a small continuous direct current to establish a nearly uniform potential variation from the A_2 to the A_3 voltage. In effect, the element constitutes a "thick" electron lens, and because there are no abrupt changes in potential, the trace-distortion effects are much smaller than in a thin lens.

5.2.3 References

1. Spangenberg, K. R., *Vacuum Tubes*, McGraw-Hill, New York, N.Y., 1948.
2. Sherr, S.: *Fundamentals of Display Systems Design*, Wiley, New York, N.Y., 1970.
3. Cloz, R., et al.: "Mechanism of Thin Film Electroluminescence," *Conference Record*, SID Proceedings, Society for Information Display, San Jose, Calif., vol. 20, no. 3, 1979.

5.2.4 Bibliography

Aiken, W. R.: "A Thin Cathode Ray Tube," *Proc. IRE*, vol. 45, no. 12, pp. 1599–1604, December 1957.

Barkow, W. H., and J. Gross: "The RCA Large Screen 110° Precision In-Line System," ST-5015, RCA Entertainment, Lancaster, Pa.

Casteloano, Joseph A.: *Handbook of Display Technology*, Academic, New York, N.Y., 1992.

Fink, Donald, (ed.): *Television Engineering Handbook*, McGraw-Hill, New York, N.Y., 1957.

Fink, Donald, and Donald Christiansen (eds.): *Electronics Engineers Handbook*, 3rd ed., McGraw-Hill, New York, N.Y., 1989.

Hutter, Rudolph G. E., "The Deflection of Electron Beams," in *Advances in Image Pickup and Display*, B. Kazan (ed.), vol. 1, pp. 212–215, Academic, New York, N.Y., 1974.

Jordan, Edward C. (ed.): *Reference Data for Engineers: Radio, Electronics, Computer, and Communications*, 7th ed., Howard W. Sams, Indianapolis, IN, 1985.

Morell, A. M., et al.: "Color Television Picture Tubes," in *Advances in Image Pickup and Display*, vol. 1, B. Kazan (ed.), pg. 136, Academic, New York, N.Y., 1974.

Pender, H., and K. McIlwain (eds.), *Electrical Engineers Handbook*, Wiley, New York, N.Y., 1950.

Popodi, A. E., "Linearity Correction for Magnetically Deflected Cathode Ray Tubes," *Elect. Design News*, vol. 9, no. 1, January 1964.

Sherr, S.: *Electronic Displays*, Wiley, New York, N.Y. 1979.

Sinclair, Clive: "Small Flat Cathode Ray Tube," *SID Digest*, Society for Information Display, San Jose, Calif., pp. 138–139, 1981.

Zworykin, V. K., and G. Morton: *Television*, 2d ed., Wiley, New York, N.Y., 1954.

Chapter

5.3 Electromagnetic Deflection

Sol Sherr

5.3.1 Introduction

In contrast with electrostatic deflection systems, the components in an electromagnetic deflection system are almost universally located outside the tube envelope, rather than inside the vacuum. Because the neck of the CRT beyond the electron gun is free of obstructions, a larger-diameter electron beam can be used in the magnetic deflection CRT than in the electrostatic deflection device. This permits greater beam current to the phosphor screen and, consequently, a brighter picture. Deflection angles of 110° (55° off-axis) are commonly used in video display tubes without excessive spot defocusing. Large deflection angles permit the CRT to be constructed with a shorter bulb section for a given screen size.

The electromagnetic deflection yoke is most suitable for repetitive types of scanning, such as raster scans in which parallel scan lines are swept out in a rectangular area. The yoke is also well suited for *plan-position-indicator* (PPI) scans in which a radial scan line is directed outward from the center of the screen to cover a circular area.

Electromagnetic deflection has also been used for random address displays. The principal design challenge with random deflection is the inductance of the deflection coils. For any specific field strength an ampere-turns product must be established. Therefore, low inductance implies high current, which may be difficult to supply, especially for large bandwidth signals. Normally, for each axis the yoke includes two coils, each bent into a saddle shape and extending halfway around the CRT neck.

PPI deflection may be accomplished with a single axis yoke that is rotated physically by an external motor, or self-synchronous repeater driven by the radar antenna. With this arrangement, a constant-amplitude triggered linear-sawtooth wave is applied to the yoke. Another approach to PPI deflection employs a stationary yoke with two orthogonal deflection axes. One axis receives a current waveform of the linear sawtooth with its amplitude coefficient varying according to the algebraic sine of the antenna rotation angle; the other axis receives a similar waveform, varying according to the algebraic cosine of the rotation angle.

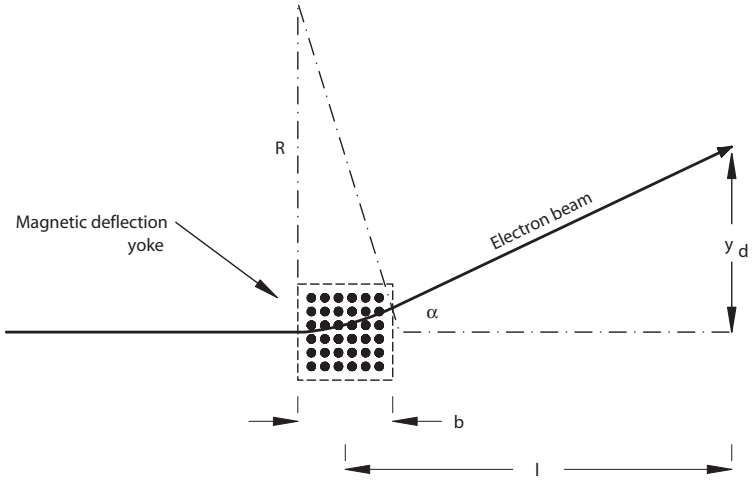

Figure 5.3.1 Principle quantities of magnetic deflection. (*After* [2].)

5.3.2 Principles of Operation

The basic magnetic deflection equation is derived from the expression of the behavior of an electron stream in the presence of a magnetic field [1]. For a uniform magnetic field, the radius r of the electron path when the electron enters the field at right angles is given by

$$r = \frac{3.38 \times 10^{-6} V^{1/2}}{B_m} \quad \text{m} \tag{5.3.1}$$

Where:
B_m = magnetic flux density
V = potential at initial velocity

Figure 5.3.1 illustrates the basic parameters of electron beam deflection by a magnetic field. Assuming that the magnetic field is uniform within the area delineated by the dots, the electron beam will follow the arc of a circle whose radius R is given by

$$R = \frac{3.38 \times 10^{-6} V^{1/2} \sin\theta}{B_m} \tag{5.3.2}$$

where θ = the angle at which the electron enters the field.

The angle at which the beam leaves the magnetic field is then given by

$$\sin\alpha = 2.97\times10^{5}\,\frac{l\,B_m}{V^{1/2}} \tag{5.3.3}$$

The deflection is related to this angle by

$$yd = l\tan\alpha \tag{5.3.4}$$

tan α is approximately equal to *yd*/*l* because the center of deflection is at the center of the field. Substituting terms provides

$$yd = 2.97\times10^{5}\,\frac{l^2\,B_m}{V^{1/2}} \tag{5.3.5}$$

This equation assumes that sin α, tan α, α and α are all equivalent, which holds true for the small values of α. For cases where this equivalence does not hold, the deflection is not directly proportional to the current because sin α rather than tan α is proportional to the current. This leads to the need for corrective circuitry to compensate for the error.

5.3.2a Flat-Face Distortion

Flat-face distortion results from the difference between the radius of curvature of the deflected beam and the actual radius of the display surface [1]. This distortion is illustrated in Figure 5.3.2 for the general case. The ratio of true deflection to deflection on an ideal surface that has its deflection center at the center of curvature, is given by

$$\frac{d_a}{d_i} = \frac{R_a\sin\theta_a}{R_i\sin\theta_i} \tag{5.3.6}$$

The deflection angle may be expressed in terms of current through the yoke by substituting for B_m in the equation that describes the angle at which an electron beam leaves a magnetic field (which follows) and using a constant to replace all other terms.

$$\sin\alpha = 2.97\times10^{5}\,\frac{l\,B_m}{V^{1/2}} \tag{5.3.7}$$

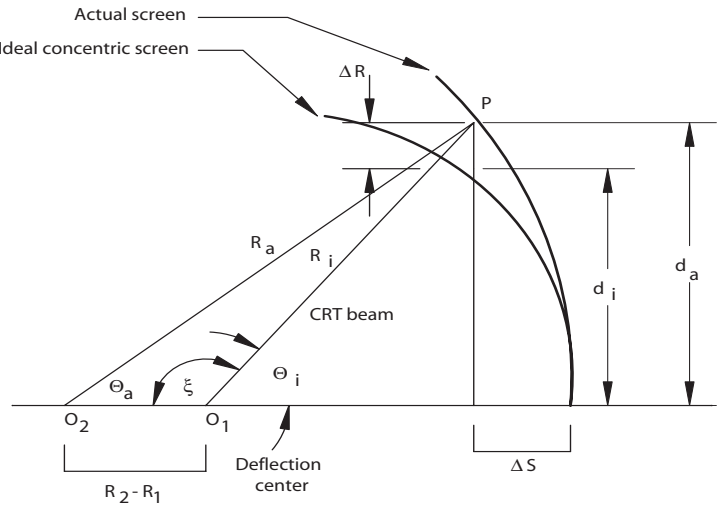

Figure 5.3.2 Linearity distortion resulting from CRT screen curvature. (*After* [3].)

After making the substitutions described, including substituting θ for α, the equation becomes

$$\sin\theta = KI \tag{5.3.8}$$

It is clear that only in the ideal case will the deflection be directly proportional to the yoke current. If the general case is then applied to the specific case of the flat-faced screen, as illustrated in Figure 5.3.3, the equation becomes

$$\frac{d_a}{d_i} = \frac{R_a \tan\theta}{R_a \sin\theta} \tag{5.3.9}$$

The equation can be simplified to

$$\frac{d_a}{d_i} = \frac{1}{\cos\theta} \tag{5.3.10}$$

If the equation is rewritten as

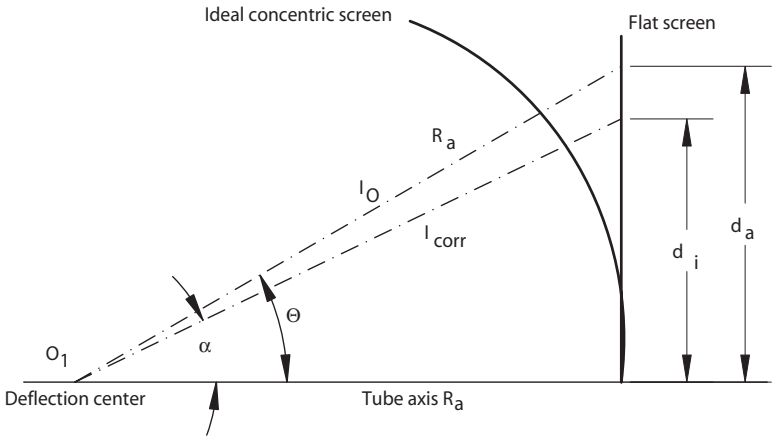

Figure 5.3.3 The mechanics of flat-face CRT linearity distortion. (*After* [4].)

$$\frac{d_a}{d_i} = \frac{1}{\left(1-\sin^2\theta\right)^{1/2}} \tag{5.3.11}$$

it may be further reduced by using the equation

$$\sin\theta = KI \tag{5.3.12}$$

(described previously). By then expanding the denominator, the following results (if all but the first two terms of the expansion are neglected):

$$d_a = d_i\left\{1+\frac{K^2 I^2}{2}\right\} \tag{5.3.13}$$

The resulting indicated deflection error can be compensated for dynamically by introducing special compensation circuitry.

5.3.2b Deflection Defocusing

Another effect resulting from deflection of the electron beam is the defocusing that occurs when the beam is moved from the center to some other location on the CRT screen [1]. The changes in focus result from the edges of the beam entering the magnetic field at different angles because of

convergence. The edges of the beam will be deflected by the same radius of curvature and leave the field with a new convergence angle. This effect can be reduced through the use of dynamic focusing circuits.

5.3.2c Deflection Yoke

In order to understand the operation and function of the deflection yoke, it is necessary to examine its underlying structure. The definition of field strength is given by

$$H D_a = ni \tag{5.3.14}$$

Where:
H = field strength (H)
D_a = yoke diameter (m)
n = number of turns
i = current through the yoke (A)

The length of the field is expressed by [5]

$$l = r \sin\theta \tag{5.3.15}$$

Where:
l = length of the uniform magnetic field
r = radius of the electron path
θ = the deflection angle

The dimensions of the yoke are set by the maximum deflection angle and the outside diameter of the CRT neck. These establish the maximum length and minimum inside diameter of the yoke. Given these parameters and the accelerating voltage of the CRT, supporting math may be reduced to provide a simple relationship between the yoke inductance and current:

$$k = \frac{L I^2}{2} \tag{5.3.16}$$

Where:
k = the yoke energy constant for a given deflection angle and accelerating voltage (μs)
L = yoke inductance (μH)
I = yoke current (A) to deflect the beam through the half-angle selected by accelerating voltage

The maximum voltage induced across the yoke is found from

$$e = L\frac{di}{dt} \tag{5.3.17}$$

Where:
e = the induced potential (V)
L = yoke inductance (H)
di/dt = rate of change of current (A/s)

Another factor that determines the upper operating limit for the yoke is the *retrace time*, which must be less than the approximately 10 μs allowed for NTSC video. The natural retrace time for a yoke can be found from

$$T_r = \pi\left(L_y C_y\right)^{1/2} \leq 10\,\mu\text{s} \tag{5.3.18}$$

Where:
L_y = yoke inductance (H)
C_y = yoke capacitance (F)
T_r = retrace time (s)

Using a shunt capacitance value of 330 pF leads to a maximum yoke inductance of 30 mH. This applies to the horizontal-deflection yoke. The vertical-deflection yoke can be larger because of the longer retrace time of about 2 ms for NTSC, leading to yoke inductances as high as 1 H.

For a specific yoke with a constant anode voltage, the current required for deflection varies as the sine of the deflection angle:

$$\frac{I_2}{I_1} = \frac{\sin\theta_2}{\sin\theta_1} \tag{5.3.19}$$

It follows that

$$I_2 = I_1\frac{\sin\theta_2}{\sin\theta_1} \tag{5.3.20}$$

Where:
I_1 = the given current
I_2 = new current
θ_1 = the given deflection angle
θ_2 = the new deflection angle

If the deflection yoke is given, and the deflection angle is constant, then the deflection current will vary as the square root of the anode voltage:

$$\frac{I_2}{I_1} = \left\{\frac{V_2}{V_1}\right\}^{1/2} \tag{5.3.21}$$

Where:
V_1 = the given anode voltage
V_2 = new anode voltage

The step response of the yoke can be found from [4]

$$I = \frac{E}{R\left\{1 - e^{(-Rt/L)}\right\}} \tag{5.3.22}$$

Where:
E = the voltage across the yoke
R = yoke resistance
t = settling time
I = current through the yoke
L = yoke inductance

If R/L is considerably smaller than 1, this equation reduces to

$$I = \frac{E\,R\,t}{R\,L} \tag{5.3.23}$$

It can be further simplified to

$$t = \frac{I\,L}{E} \tag{5.3.24}$$

This commonly used equation for *settling time* is accurate to about 1 percent for settling time to 99 percent of the final value. However, it may be in error by as much as 25 percent for settling time to 99.9 percent of the final value, or if R/L is not sufficiently small. However, it is usually adequate for most calculations and is in general use.

All the proportionalities of yoke application may be combined in a single equation

$$I_2 = I_1 \left\{ \frac{L_1}{L_2} \right\}^{1/2} \left\{ \frac{E_2}{E_1} \right\}^{1/2} \frac{\sin\theta_2}{\sin\theta_1} \tag{5.3.25}$$

Yoke Selection Parameters

The selection of a yoke for a given application involves the consideration of a number of parameters, some of which require design tradeoffs. The typical selection procedure includes the following steps:

- Select a CRT and determine the maximum deflection angle
- Determine yoke inside diameter (ID) dimensions from the CRT neck size
- Find the yoke energy constant from the yoke manufacturer, based on the ID and deflection angle
- Establish the anode voltage
- Determine the half-angle deflection for the two axes
- Calculate the energy constants
- Set the minimum time for the half-angle deflection
- Find the maximum allowable induced voltage
- Calculate the maximum allowable yoke inductance

For any given application, a number of choices usually exist, although some may be more practical to realize in hardware than others.

5.3.3 References

1. Sherr, S.: *Electronic Displays*, Wiley, New York, N.Y., 1979.
2. Spangenberg, K. R.: *Vacuum Tubes*, McGraw-Hill, New York, N.Y., 1948.
3. Popodi, A. E.: "Linearity Correction for Magnetically Deflected Cathode Ray Tubes," *Elect. Design News*, vol. 9, no. 1, January 1964.
4. Sherr, S.: *Fundamentals of Display Systems Design*, Wiley, New York, N.Y., 1970.
5. Fink, Donald (ed.): *Television Engineering Handbook*, McGraw-Hill, New York, N.Y., 1957.

5.3.4 Bibliography

Aiken, W. R.: "A Thin Cathode Ray Tube," *Proc. IRE*, vol. 45, no. 12, pp. 1599–1604, December 1957.

Barkow, W. H., and J. Gross: "The RCA Large Screen 110° Precision In-Line System," ST-5015, RCA Entertainment, Lancaster, Pa.

Casteloano, Joseph A.: *Handbook of Display Technology*, Academic, New York, N.Y., 1992.

Fink, Donald, and Donald Christiansen (eds.): *Electronics Engineers Handbook*, 3rd ed., McGraw-Hill, New York, N.Y., 1989.

Hutter, Rudolph G. E.: "The Deflection of Electron Beams," in *Advances in Image Pickup and Display*, B. Kazan (ed.), vol. 1, pp. 212–215, Academic, New York, N.Y., 1974.

Jordan, Edward C. (ed.): *Reference Data for Engineers: Radio, Electronics, Computer, and Communications*, 7th ed., Howard W. Sams, Indianapolis, IN, 1985.

Morell, A. M., et al.: "Color Television Picture Tubes," in *Advances in Image Pickup and Display*, vol. 1, B. Kazan (ed.), pg. 136, Academic, New York,N.Y., 1974.

Pender, H., and K. McIlwain (eds.): *Electrical Engineers Handbook*, Wiley, New York, N.Y., 1950.

Sinclair, Clive: "Small Flat Cathode Ray Tube," *SID Digest*, Society for Information Display, San Jose, Calif., pp. 138–139, 1981.

Zworykin, V. K., and G. Morton: *Television*, 2d ed., Wiley, New York, N.Y., 1954.

Chapter

5.4 Distortion Correction Circuits

Sol Sherr

5.4.1 Introduction

The real-world restrictions of manufacturing tolerances and practical deflection systems result in devices that deviate from the ideal case. This deviation usually requires external correction circuitry to permit the device to operate within tolerances demanded by the end-user. Depending on the type of vacuum device and the intended application, one or more correction signals may be applied to the deflection elements.

5.4.2 Flat-Face Distortion Correction

The theoretical basis for flat-face distortion is defined by [1]

$$\frac{d_a}{d_i} = \frac{R_a \sin\theta_a}{R_i \sin\theta_i} \tag{5.4.1}$$

This equation, the variables of which are specified in Figure 5.4.1, specifies the ratio of the true deflection to the deflection on an ideal surface that has its deflection center at the center of curvature. This distortion may be minimized through the use of special correction circuits. The departure from linearity (illustrated in Figure 5.4.2) leads to the correction equation

$$d_a = d_i \left\{ 1 + \frac{K^2 I^2}{2} \right\} \tag{5.4.2}$$

Linearity correction can be achieved by using a circuit that compensates for the second term of the preceding equation (d_i). When rewritten by substituting KI for d_i the following statement results:

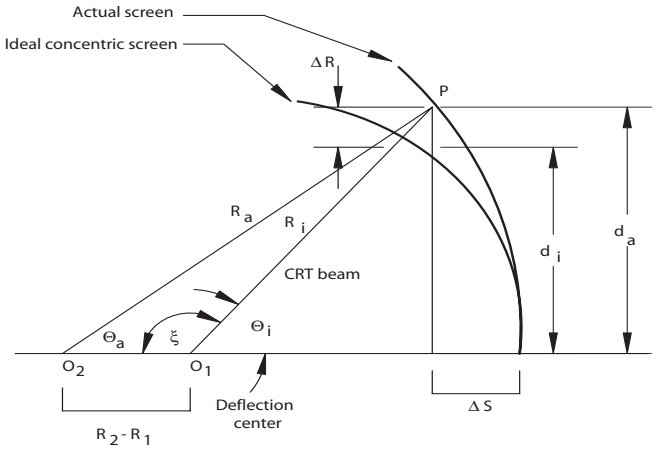

Figure 5.4.1 Linearity distortion resulting from CRT screen curvature. (*After* [2].)

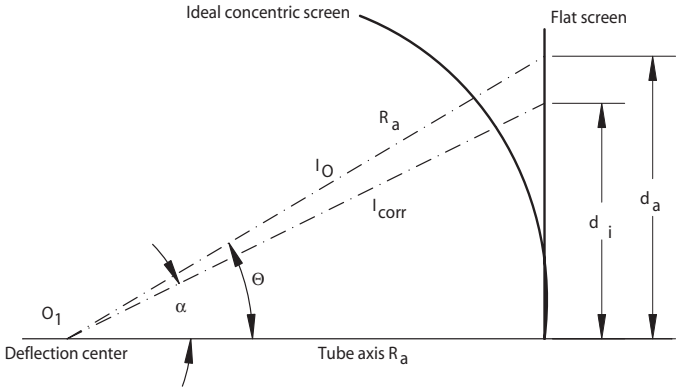

Figure 5.4.2 The mechanics of flat-face CRT linearity distortion. (*After* [1].)

$$d_a = K\,I + \left\{\frac{K^3\,I^3}{2}\right\} \tag{5.4.3}$$

Because $d_i = KI$, the second term in the equation must be subtracted to achieve linearity, with the same type of correction applied to both the X and the Y axes. This is done by obtaining the current for each axis from the yoke winding and using the type of circuit shown in Figure 5.4.3.

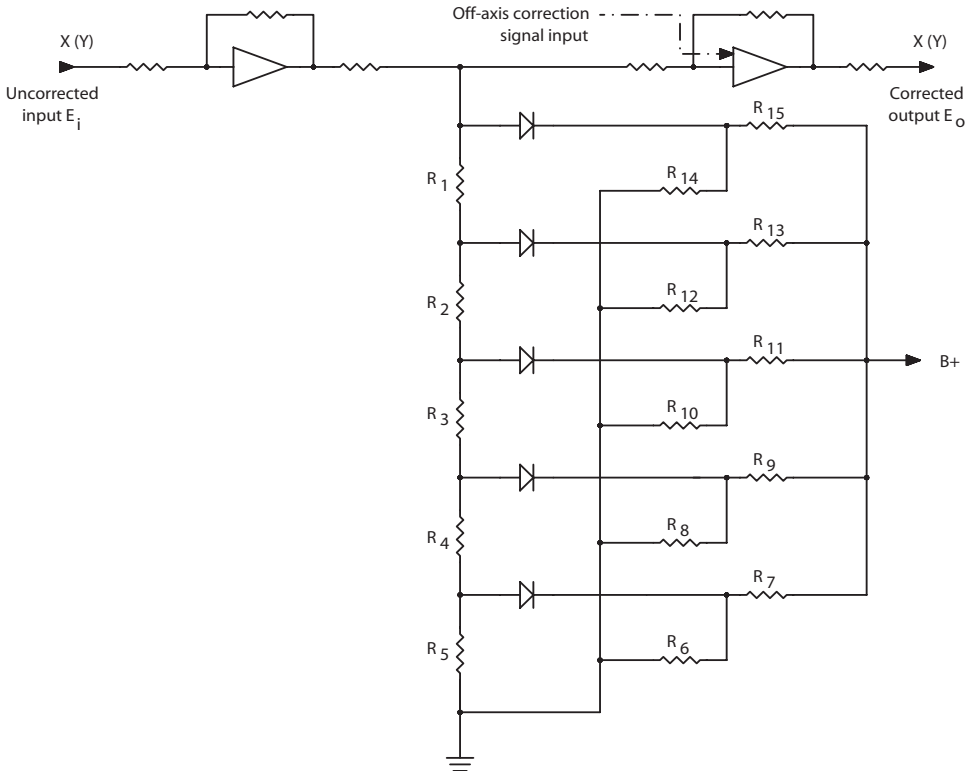

Figure 5.4.3 Basic linearity correction circuit for a CRT. (*After* [1].)

The cubic term is generated by means of a piecewise approximation, using as many diodes as necessary to achieve the desired accuracy of correction. Ten segments are usually sufficient, although only five are shown in the figure for simplicity. The circuit operates by biasing the diodes to different voltages so they will conduct only when the output of the first summing amplifier exceeds the voltages. The diode currents are then summed in the output amplifier. The output voltage is given by

$$E_o = \frac{E_i R_f}{R_p} \tag{5.4.4}$$

Where:
R_p = the equivalent value of the summing resistors
E_i = uncorrected input voltage (see Figure 5.4.3)
E_o = corrected output voltage (Figure 5.4.3)

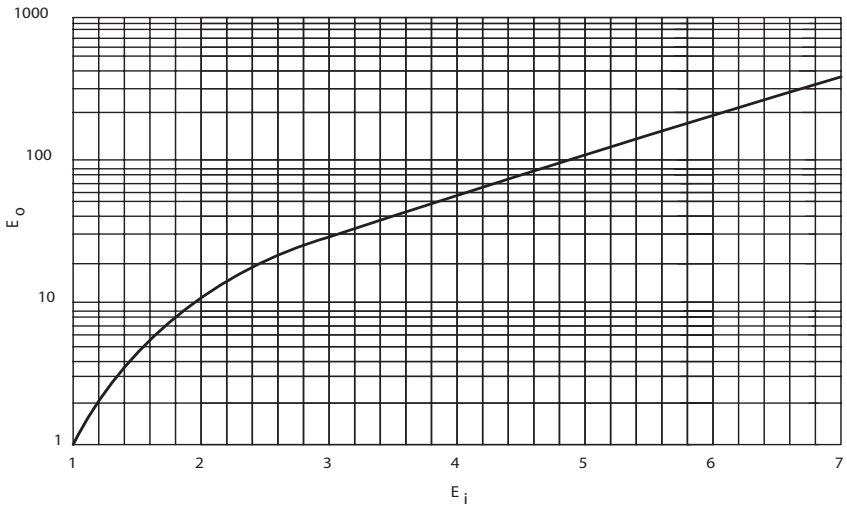

Figure 5.4.4 A plot of E_o versus E_i where $E_o = KI^3$. (*After* [1].)

The similarity to a digital-to-analog (D/A) converter is apparent, but the resistors are not binary weighted, and E_i depends on the current in the yoke. The values for R_n in the resistor network may be determined by plotting

$$E_o = K I^3 \tag{5.4.5}$$

This plot is shown in Figure 5.4.4. From this plot a piecewise approximation can be made, reading the bias levels from the horizontal axis where a new segment begins, and deriving the summing resistor values from the slope of the segment. A fairly accurate result may be attained by choosing R1 to R5 (in Figure 5.4.3) with each increasing by a factor of 2 from the previous one so that the resistors are defined by $R_n/2^n$, where n takes on the values from zero to the maximum number of segments (minus one).

The network shown in Figure 5.4.3 corrects only for on-axis nonlinearity. However, when both X and Y deflection signals are present, they will affect each other. Therefore, it is necessary to cross couple the two inputs (as shown in Figure 5.4.5).

5.4.3 Dynamic Focusing

The effect of deflection on the focus of the electron beam can be minimized by means of a correction circuit. A typical approach is shown in Figure 5.4.6. The circuit operates on the basis that the diameter of the electron beam is affected by the deflection distance on the face of the CRT, given by

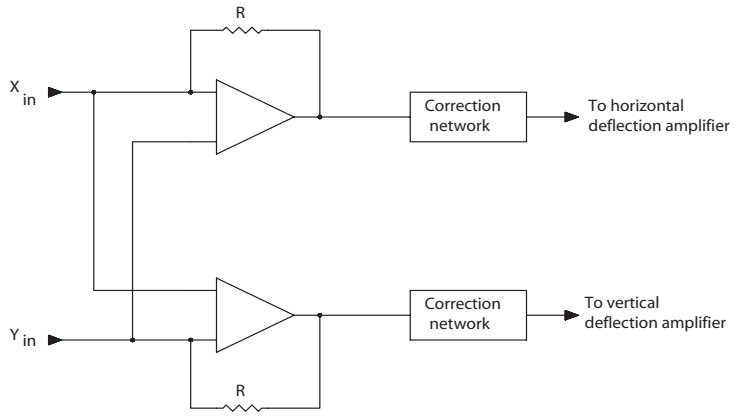

Figure 5.4.5 Block diagram of *X*/*Y* linearity correction circuit. (*After* [1].)

$$r_s = K\,d^2 \tag{5.4.6}$$

Where:
r_s = the change in spot size
d = deflection distance
K = a constant

The deflection from the center d consists of the X and Y components, and it is given by

$$d^2 = X^2 + Y^2 \tag{5.4.7}$$

The correction signal requires that the X and Y terms be generated and then summed. The square functions are produced by piecewise approximations using a diode network similar to one used for the cubic function described in the previous section. In the Figure 5.4.6 circuit, the diode break points and the values of the summing resistors can be determined by plotting the correction signal, as shown in Figure 5.4.7, and then converting the data into the number of segments required (usually not more than five). In the case illustrated, all resistors (except the first) may have the same value, which simplifies the circuit.

After the X^2 and Y^2 functions have been attained, they are added in the output summing amplifier and applied to the focusing circuit. It is possible through the use of this type of correction scheme to maintain a spot size ratio of less than 1.5:1 over 35° of deflection instead of a variation of 3:1, which is not uncommon without correction. Thus, the use of dynamic focus correction is a necessary part of any well-designed deflection system.

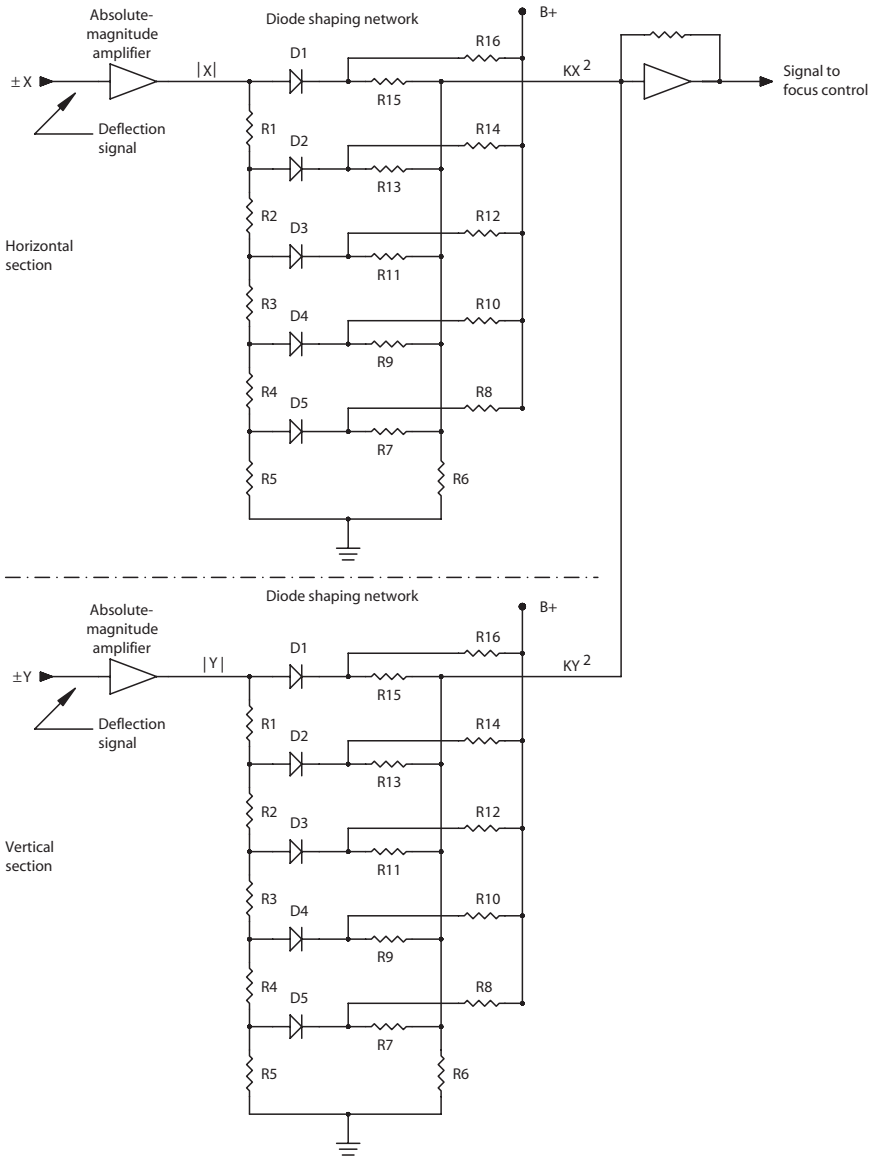

Figure 5.4.6 Basic design of a dynamic focus circuit. (*After* [1].)

5.4.4 Pincushion Correction

Pincushion distortion is illustrated in Figure 5.4.8(*a*). Pincushion correction is used in all wide-angle deflection systems. This correction may be achieved by one of the following:

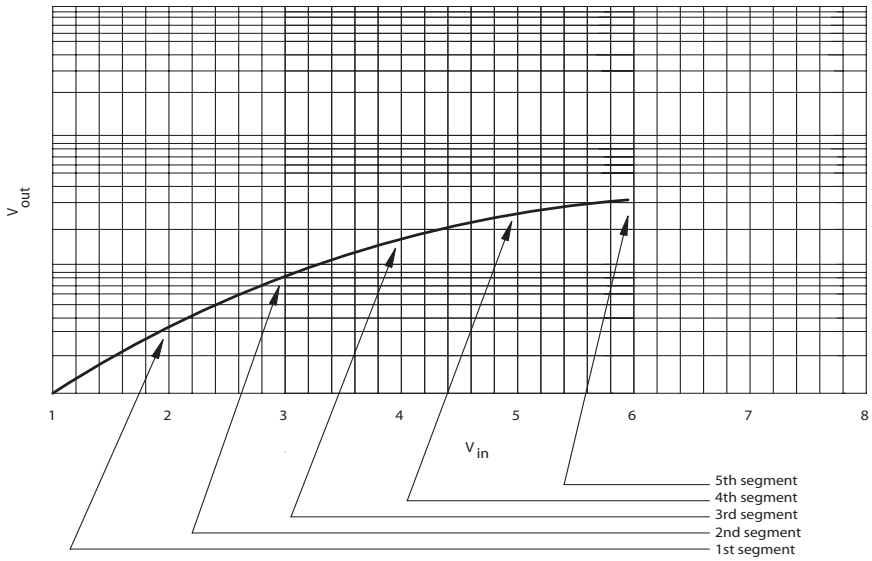

Figure 5.4.7 Plot of a dynamic focusing correction signal. (*After* [1].)

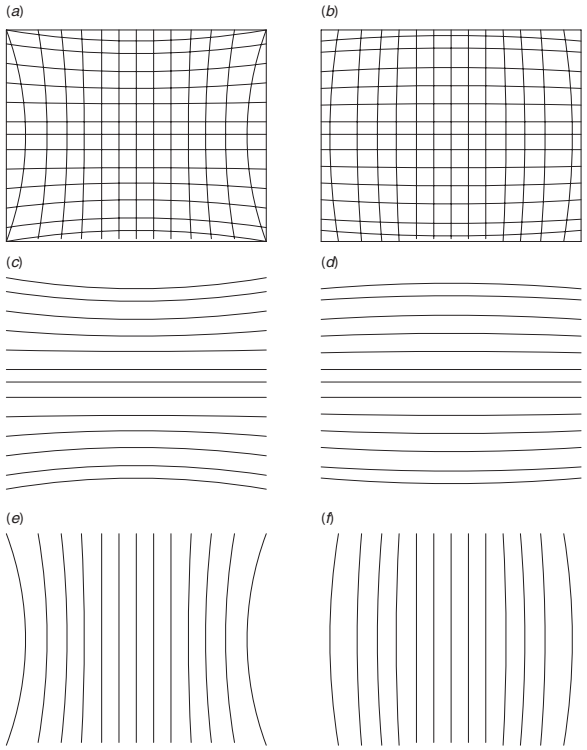

Figure 5.4.8 Pincushion distortion: (*a*) overall effect on the displayed image, (*b*) corresponding composite correction signal, (*c*) horizontal pincushion distortion component, (*d*) horizontal correction signal, (*e*) vertical pincushion distortion component, (*f*) vertical correction signal.

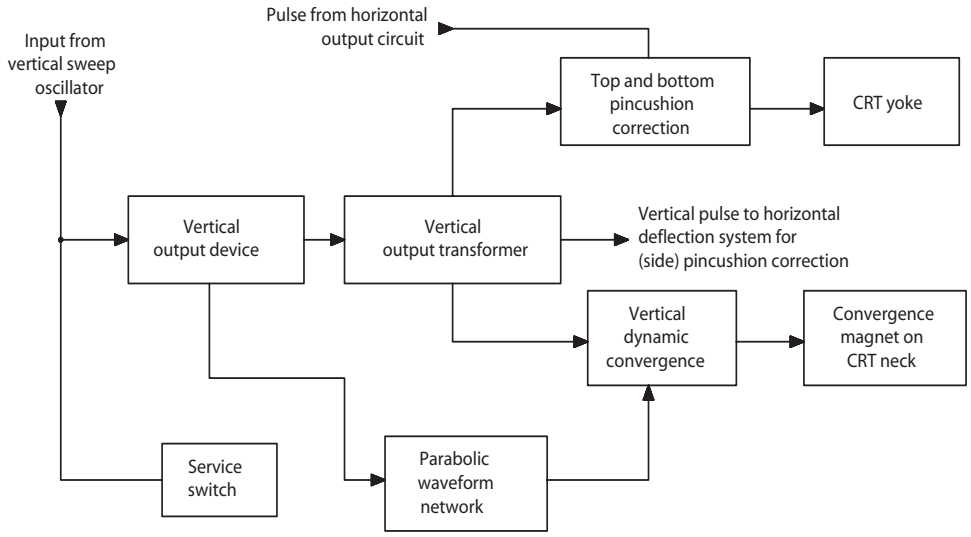

Figure 5.4.9 Block diagram of a pincushion correction circuit.

- A special yoke design that has controlled field distortion
- Predistorting the deflection current and applying it to a separate pincushion transformer that connects the correction current to the vertical yoke

The correction must compensate for the top lines shown in Figure 5.4.8 (*c*), which bow down, and the bottom lines, which bow up. The center line is straight. The corresponding correction to the raster is achieved by introducing a parabolic waveform to the vertical deflection signal, as shown in Figure 5.4.8(*d*). The vertical deflection signal is modulated by the parabolic correction waveform at the horizontal deflection rate. It is then combined with the vertical deflection system output to produce the corrected vertical deflection signal. A block diagram of such a system is shown in Figure 5.4.9.

Side correction is another form of pincushion compensation. The distortion to be corrected occurs in the vertical dimension, as shown in 5.4.8(*e*). In this case, the vertical deflection current modulates the horizontal deflection signal at the vertical scanning frequency. To accomplish this task, the vertical signal is modified by an RC network (or by an equivalent means) to produce the desired correction wave shape, which is then applied through a pincushion transformer to the horizontal yoke.

5.4.5 Multiple-Beam Dynamic Convergence

Dynamic convergence is an essential requirement for delta-gun CRT-based display systems. In-line tubes, which use predistortion in the deflection yokes for this purpose, do not require dynamic convergence of the type described in this section. However, it is useful to understand the

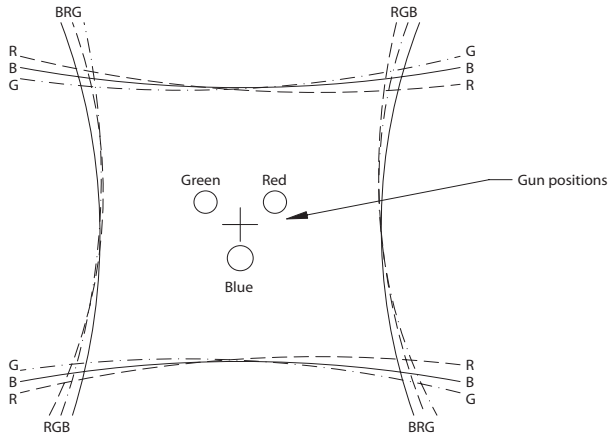

Figure 5.4.10 The effect of beam parallax. (*After* [5].)

effects that cause misconvergence when the beam is swept through angles of 70° and more. These distortions occur as the result of two effects:

- *Beam parallax*, where the beams are off axis when they arrive at the deflection yoke
- *Beam tilt*, where the beams contain a component of radial velocity as the result of being converged before deflection

The effect of beam parallax is shown in Figure 5.4.10 where, with the three guns arranged as illustrated, the three sweeps take on rhombic patterns. The effect of beam tilt is shown in Figure 5.4.11, and from the triangle A, D, Q it follows that

$$\sin(\alpha+\beta) = K(i_d + i_0) \tag{5.4.8}$$

Where:
K = a constant
i_d = deflection current
i_0 = direct current = sin β/K

The dc term may be either positive or negative, depending on the sine and amplitude of the convergence angle β, and displaces the beams as shown in Figure 5.4.12. It is evident from the figure that the green beam is leading, and the red is trailing the blue beam, with the resultant shifts illustrated by the patterns shown in Figure 5.4.13. Correction can be achieved by generating parabolic waveforms of the type shown in Figure 5.4.14. The waveforms can then be applied to the deflection yokes to achieve dynamic convergence.

Alternatively, a special convergence yoke can be included. In either case, this discussion is primarily of historical interest, because in-line guns and predistorted yokes have essentially eliminated the need for separate dynamic-convergence circuits or yokes.

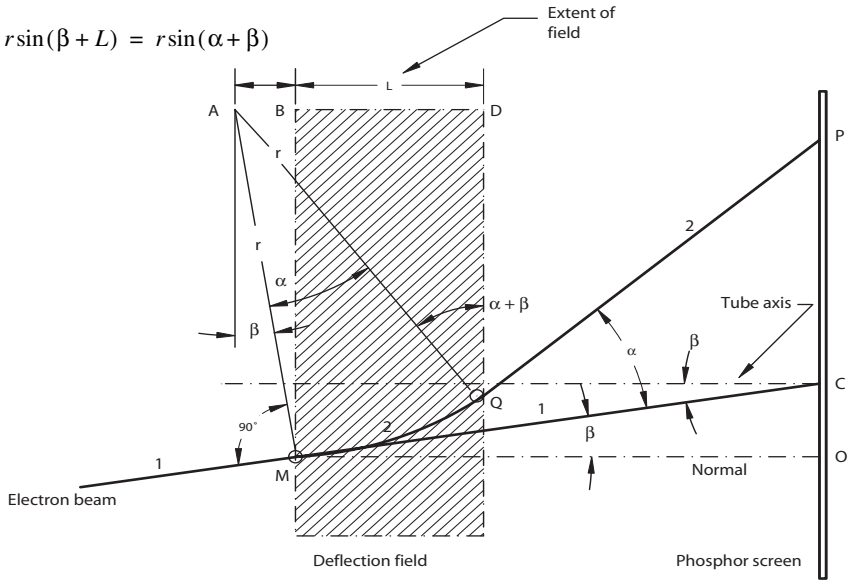

Figure 5.4.11 The effect of beam tilt. (*After* [4].)

5.4.5a In-Line System Convergence

By providing nonuniform fields to overcome the basic overconvergence of in-line beams that are statically converged at the center, in-line display systems eliminate the need for special circuits and convergence yokes. These beams, when deflected, cross over before they reach the screen, as is shown in Figure 5.4.15. By using a self-converging yoke, nonuniform fields are generated that balance the overconvergence by causing the beams to diverge horizontally inside the yoke, so that the horizontal yoke generates a pincushion-shaped field with its intensity increasing as the horizontal distance from the axis increases. Similarly, the vertical yoke creates a barrel-shaped field that diverges the beams horizontally. Thus, the self-converging yoke causes almost perfect vertical-line focus along the axis because of the horizontal-negative and vertical-positive isotropic astigmatism. In addition, the anisotropic astigmatism is removed and the coma resulting from the yoke is eliminated in the gun. However, this self-convergence without any dynamic convergence is effective only in small-angle (90°) systems. For 110° systems there is a small systematic convergence error that can be overcome by limiting it to the horizontal and using only one scanning frequency for correction. This may be achieved by either of the two techniques shown in Figure 5.4.16. In either system, the horizontal lines converge over the whole raster, and the vertical lines converge along the horizontal axis. Convergence is achieved by means of quadripole windings on the yoke that are energized by one scanning frequency.

The in-line system with self-convergence along the horizontal axis results in better convergence and requires only vertical frequency correction current, which is less expensive and results in less deflection defocusing. The net result is improved convergence with only two preset dynamic controls. At the same time, the yoke is more compact and sensitive, and the CRT is shorter by about 10 mm.

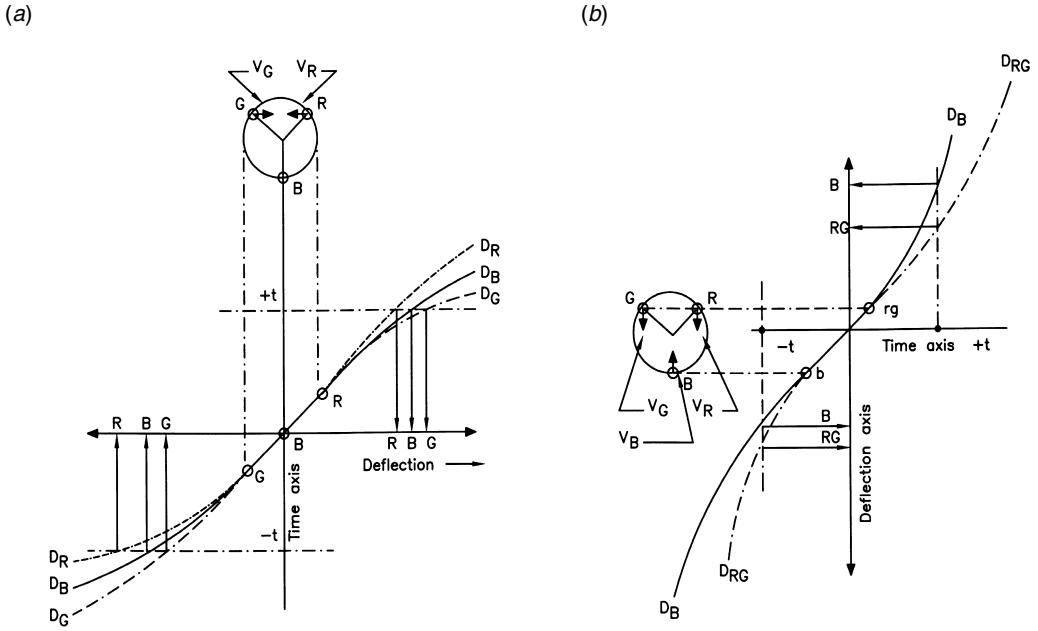

Figure 5.4.12 Color dot displacement: (*a*) horizontal deflection, (*b*) vertical deflection. (After [5].)

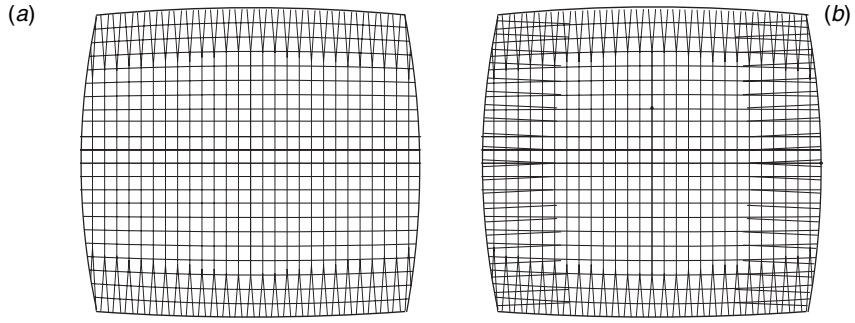

Figure 5.4.13 Color dot displacement: (*a*) horizontal shift of vertical green bars, (*b*) vertical shift of horizontal blue bars. (*After* [5].)

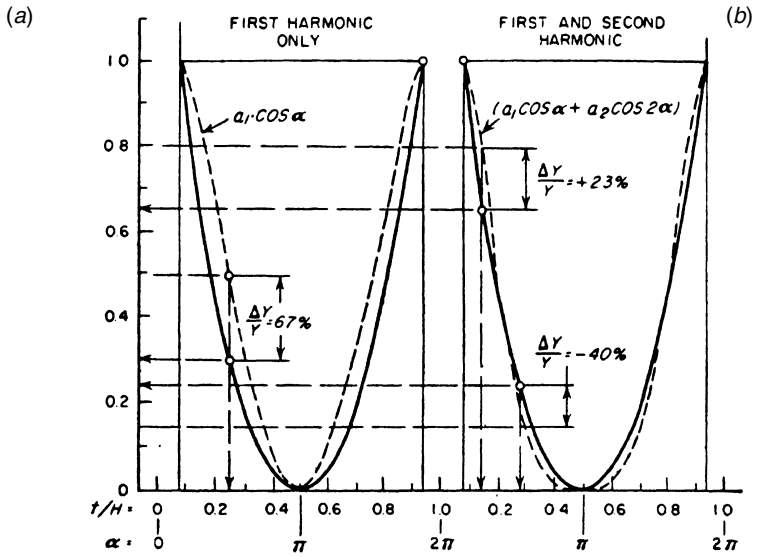

Figure 5.4.14 Parabolic correction waveforms: (*a*) first harmonic only, (*b*) first and second harmonic signals.

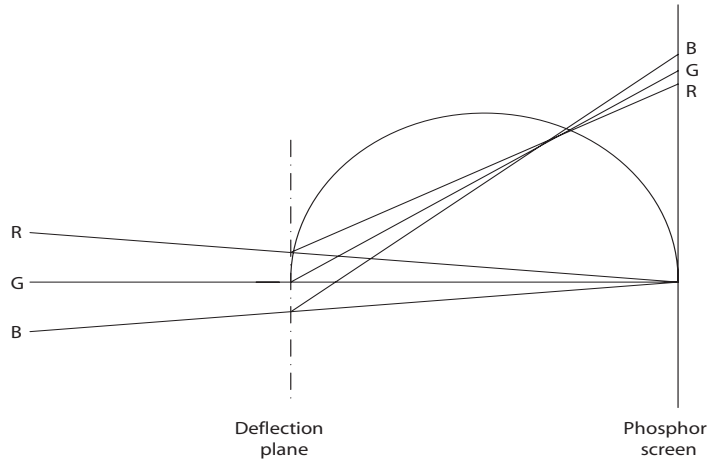

Figure 5.4.15 The image field showing beam crossover. (*After* [3].)

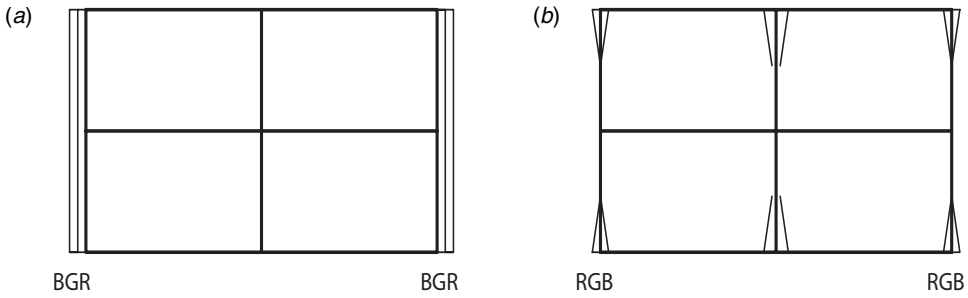

Figure 5.4.16 Self-converging in-line system: (*a*) vertical, (*b*) horizontal. (*After* [3].)

5.4.6 References

1. Sherr, S.: *Fundamentals of Display Systems Design*, Wiley, New York, N.Y., 1970.
2. Popodi, A. E.: "Linearity Correction for Magnetically Deflected Cathode Ray Tubes," *Elect. Design News*, vol. 9, no. 1, January 1964.
3. Barkow, W. H., and J. Gross: "The RCA Large Screen 110° Precision In-line System," ST-5015, RCA Entertainment, Lancaster, Penn.
4. Dasgupta, B. B.: "Recent Advances in Deflection Yoke Design," *SID International Symposium Digest of Technical Papers*, Society for Information Display, San Jose, Calif., pp. 248–252, May 1999.
5. Fink, Donald (ed.): *Television Engineering Handbook*, McGraw-Hill, New York, N.Y., 1957.

5.4.7 Bibliography

Aiken, W. R.: "A Thin Cathode Ray Tube," *Proc. IRE*, vol. 45, no. 12, pp. 1599–1604, December 1957.

Barkow, W. H., and J. Gross: "The RCA Large Screen 110° Precision In-Line System," ST-5015, RCA Entertainment, Lancaster, Pa.

Casteloano, Joseph A.: *Handbook of Display Technology*, Academic, New York, N.Y., 1992.

Fink, Donald, and Donald Christiansen (eds.): *Electronics Engineers Handbook*, 3rd ed., McGraw-Hill, New York, N.Y., 1989.

Hutter, Rudolph G. E.: "The Deflection of Electron Beams," in *Advances in Image Pickup and Display*, B. Kazan (ed.), vol. 1, pp. 212–215, Academic, New York, N.Y., 1974.

Jordan, Edward C. (ed.): *Reference Data for Engineers: Radio, Electronics, Computer, and Communications*, 7th ed., Howard W. Sams, Indianapolis, IN, 1985.

Morell, A. M., et al.: "Color Television Picture Tubes," in *Advances in Image Pickup and Display*, vol. 1, B. Kazan (ed.), pg. 136, Academic, New York,N.Y., 1974.

Pender, H., and K. McIlwain (eds.), *Electrical Engineers Handbook*, Wiley, New York, N.Y., 1950.

Sinclair, Clive: "Small Flat Cathode Ray Tube," *SID Digest*, Society for Information Display, San Jose, Calif., pp. 138–139, 1981.

Zworykin, V. K., and G. Morton: *Television*, 2d ed., Wiley, New York, N.Y., 1954.